



ELSEVIER

Journal of Volcanology and Geothermal Research 100 (2000) 289–320

Journal of volcanology
and geothermal research

www.elsevier.nl/locate/jvolgeores

Temporal gravity at Merapi during the 1993–1995 crisis: an insight into the dynamical behaviour of volcanoes

P. Jousset^{a,b,*}, S. Dwipa^c, F. Beauducel^d, T. Duquesnoy^e, M. Diament^a

^aLaboratoire de Gravimétrie et Géodynamique (J.E. 335), Institut de Physique du Globe de Paris, Case 89, 4 Place Jussieu, 75252 Paris Cedex 05, France

^bCentre de Recherche en Géophysique, École des Mines de Paris, 35 rue St Honoré, 77305 Fontainebleau Cedex, France

^cVolcanological Survey of Indonesia, Bandung 40122, Indonesia

^dDépartement de Sismologie (URA 195 du CNRS), Institut de Physique du Globe de Paris, France

^eInstitut Géographique National, LOEMI, Saint-Mandé 94160, France

Abstract

Gravity signals were recorded during volcanic activity of Merapi volcano between 1993 and 1995. First we repeated measurements of gravity (with Scintrex CG3-M) and of elevation (with GPS receivers) on a network. Within this period, we observed little deformation (less than 5 cm), but significant gravity changes (up to almost +400 μGal and $-270 \mu\text{Gal}$). The growth of the dome explains most of the gravity signal. However, a residual gravity change is interpreted as an increase of 4×10^8 kg of the volcano mass, under the northwestern part of the summit. We consider and discuss several models, including non-volcanic effects (e.g. water table level change), and magmatic processes, such as the intrusion of magma, or the effect of crystallisation of implaced magma. Secondly, we installed a gravity meter in Babadan observatory, located at 4 km from the summit, which has been recording continuously since 1993. The analysis of these records leads to a precise Earth tide model for the Merapi area with an accuracy of 1.3 μGal for M_2 . We consider both the continuous monitoring of the mass movement within the volcano and the response of the volcano to the tidal potential. A correlation exists between residual drift and seismic and volcanic activity. For example, a decrease of the residual drift corresponds to intensive seismic activity (LF event) and the occurrence of nuées ardentes, whereas no remarkable activity is associated with increases of the residual drift. The admittance variations, a combination of the meter sensitivity (which is tilt-dependent) and the mechanical response of the ground to tidal forces, are also correlated to volcanic events. We propose that during 1993–1995, oscillations of the internal pressure (a few MPa) due to crystallisation and degassing magma lead to direct summit activity. © 2000 Elsevier Science B.V. All rights reserved.

Keywords: microgravity; mass transfer; continuous recording; admittance; Merapi

1. Introduction

Volcanic eruptions are related to complex magmatic processes, the understanding of which

requires both monitoring and modelling of physical and chemical aspects of these systems. Discriminating between processes is not straightforward, despite modelling (e.g. Jaupart and Allègre, 1991; Jaupart and Tait, 1995) and the many observations accumulated over the years. For example, the intrusion of new magma or the exsolution of gas within magma both imply an increase in the volume of the magma

* Corresponding author. Tel.: +33-1-6469-4918; fax: +33-1-6469-4935.

E-mail address: jousset@geophy.ensmp.fr (P. Jousset).

chamber, which may lead to the same pattern of ground deformation at surface. Models have been built (e.g. Mogi, 1958; Hagiwara, 1977a; Davis, 1986; Bonafede, 1990; Bonafede and Olivieri, 1995; Dowden et al., 1995), but they do not allow these cases to be distinguished. One variable that can allow us to discriminate between these processes is density. In addition, density variations may be in some cases the only suitable parameter to detect internal processes (like magma displacement without seismicity, Rymer et al., 1993).

Gravity and microgravity techniques give information about the underground density distribution and its variation with time. The Bouguer anomaly gives information on the internal density distribution and thus leads to the inner structure of the volcano (e.g. Rymer and Brown, 1986; Brown et al., 1987; Rousset et al., 1989; Barberi et al., 1991; Camacho et al., 1991; Froger et al., 1992; Deplus et al., 1995). Temporal microgravity studies consist of monitoring and interpreting temporal variations of the gravity field and simultaneous vertical elevation change. Moreover, microgravity also addresses the measurement of the vertical gradient of the gravity field. Basic ideas are summarised for example in Eggers (1987). Considering that data reduction removes both instrumental and tidal effects, the remaining temporal gravity changes on volcanoes are caused by the effect of elevation changes, mass redistribution and change of density, acting in concert (Fig. 1). This is summarised in the equation:

$$\Delta g_{\text{observed}} = \Delta g_{\text{Topography change}} + \Delta g_{\text{Free-air deformation}} + \Delta g_{\text{Volume change}} + \Delta g_{\text{Density change}} \quad (1)$$

where:

$\Delta g_{\text{Topography change}}$ is the gravity effect of the mass added/removed on the ground surface due to extrusion/collapse of material in the surroundings of the points;

$\Delta g_{\text{Free-air deformation}}$ is the gravity effect of elevation changes of the observation point;

$\Delta g_{\text{Volume change}}$ is the gravity effect of the global volume variation, at the observation point, generated by an increase/decrease of the volume of the volcano from an internal process, excluding added/removed mass at surface; and

$\Delta g_{\text{Density change}}$ the gravity effect due to the change of global mass inside the edifice, internal density change (e.g. groundwater level change, volcanic process) or inner mass displacement.

Two methods may be used to investigate the volcanic processes disturbing the gravity field with time:

(1) Measurements are repeated at different times at many points. The repetition network should extend from areas where the gravity field is expected to vary to areas where it is expected to be constant (Fig. 1).

(2) Continuous recording of the gravity field over a long period of time; ideally, at least two continuously recording stations are needed in order to obtain differential measures.

Previous studies have shown that microgravity changes are detectable before, during or after volcanic crises (see e.g. Jachens and Eaton, 1980; Yokoyama, 1989; Brown et al., 1987). These changes may or may not be associated with height variations and volcanic eruptions with their amplitude varying from a few to several hundred microgal ($1 \mu\text{Gal} = 10^{-8} \text{ms}^{-2}$). Moreover, the discrepancy between the theoretical value of the vertical gradient ($-306.8 \mu\text{Gal/m}$) and the measured values may be large (Poas: $-420 \mu\text{Gal/m}$; Etna: $-365 \mu\text{Gal/m}$; Breiddalur: $-201 \mu\text{Gal/m}$, all in Rymer, 1994). These measurements may enable interpretation of the magma transfer process for the inflation–deflation–inflation sequence (Rundle, 1978; Eggers, 1983; Berrino et al., 1992; Rymer and Tryggvason, 1993) or magma migration (Johnsen et al., 1980; Sanderson, 1982; Rymer et al., 1993). Other phenomena may also be involved, such as water table level change (Jachens and Roberts, 1985; Goodkind, 1986; Hunt and Kissling, 1994) and tectonic or seismic activity (Barnes, 1966; Lambert and Beaumont, 1977; Hagiwara, 1977b; Jachens et al., 1983; De la Cruz-Reyna et al., 1986). Rymer's (1994) exhaustive synthesis of the published data shows that the smallest residual gravity changes are associated with eruptions from volatile-poor basaltic magma at sites such as Kilauea (Dzurisin et al., 1980), Krafla (Torge, 1981), Etna (Sanderson, 1982; Rymer et al., 1993), Miakejima or Mihara (Iida et al., 1952; Yokoyama, 1989), whereas the largest residual values occur at explosive, subduction related stratovolcanoes built from volatile-rich andesitic magma such as Mt Baker (Malone and Frank, 1975), Pacaya

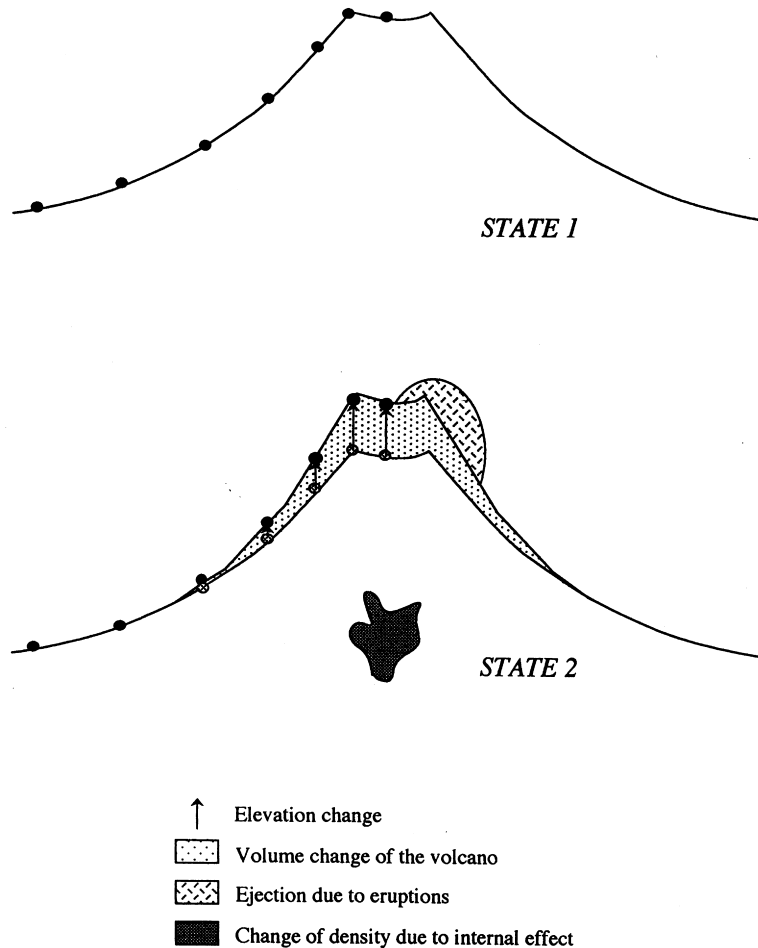


Fig. 1. Schematic temporal evolution of an active volcano. Possibilities to produce gravity changes are reported in the figure. From an initial state (state 1), where black dots represent the location of measurements point, the gravity variation at the second state (state 2) may change due to the surface movement (which involves free-air elevation change and volume change of the volcano), mass redistribution of the topography at surface (extrusions) and internal mass redistribution.

(Eggers, 1983), Mt St Helens (Jachens et al., 1984), Usu or Sakurajima (Yokoyama, 1989), Poas (Rymer and Brown, 1989) or Mayon (Jahr et al., 1995). Evidence for gravity variations at calderas has been obtained at Yellowstone (Smith et al., 1989), Rabaul Caldera (McKee et al., 1989), Campi Flegrei (Berrino et al., 1992), Askja (Brown et al., 1991; Rymer and Tryggvason, 1993) and Masaya (Bonvalot et al., 1995).

One of the main drawbacks of repeated network monitoring is that it gives only instantaneous states of the mass distribution for continuously active systems. The interval between repetition given in

published papers is about several months to more than a year. One of the smallest repeat intervals was carried out at Poas by Rymer and Brown (1987), but only for a period of several days. A promising technique to derive better information on mass transfer is continuous gravity monitoring (Goodkind, 1986) as currently tested in Timanfaya (Van Ruymbeke et al., 1994) and Etna (De Meyer et al., 1995).

Because these studies are devoted to tiny gravity variations with time, they require attention to the accuracy of the measurements and to the data reduction (Tilling, 1989).

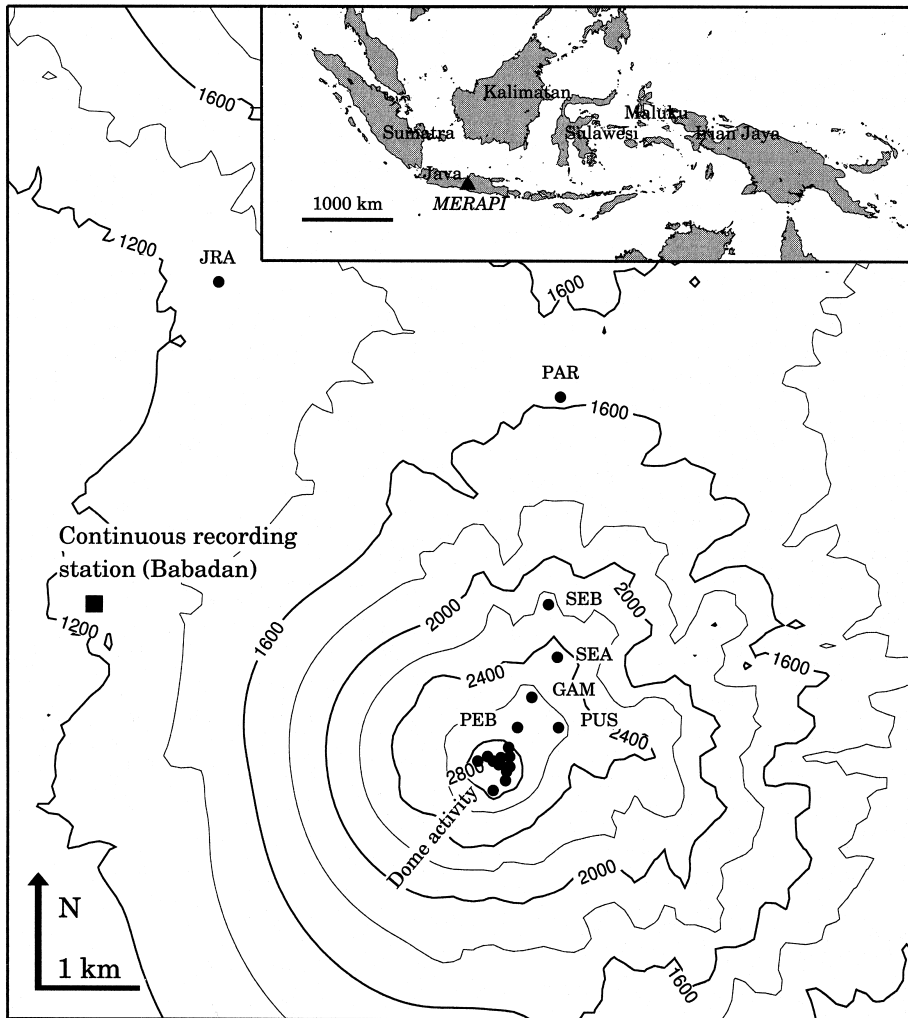


Fig. 2. Location of the repetition network points on Merapi volcano and of the continuously recording station at Babadan. Inset shows location of the Merapi volcano in Indonesia.

1. Accurate equipment is required, both for gravity and deformation measurements.
2. An accurate Earth tide model is required, because tidal effects are the same size as expected gravity changes.
3. Deformation data are required, especially elevation changes.
4. The value of the vertical gravity gradient is needed to remove properly the effect of the vertical displacement.
5. The gravitational effect of topography change is important on those volcanoes where eruptions change the topography.
6. External parameters like temperature or pressure variations, and rainfall may influence gravity data.

In this paper, we address Merapi volcano, Indonesia, an andesitic volcano belonging to a subduction arc (Fig. 2). Merapi is very active, and UNESCO declared it a Decade Volcano in 1995. It is intensively monitored by the Merapi Volcano Observatory (MVO), a department of the Volcanological Survey of Indonesia (VSI) whose objective is to mitigate its eruptions (Tjetjep, 1995). Up to now, the seismicity level and the location of earthquakes are

the main parameters used to estimate the probability of an eruption (Ratdomopurbo and Poupinet, 2000 – this volume). The only gravity studies reported so far have been for purposes of structural interpretation (Yokoyama et al., 1970; Utung and Sato, 1978; Dvorak et al., 1982; Wawan, 1985; Wahyudi, 1986; Sidik, 1989; Dwipa et al., 1994; Laesanpura, 1994; Arsadi, 1995; Jousset, 1996).

The aim of this paper is to present and interpret the results of a microgravity study carried out on Merapi volcano that involved both a network with a repeat period of one year, and continuous gravity recording, between 1993 and 1995. On the basis of this work, a model for the evolution of Merapi volcano over the two years is proposed.

2. Geological setting

Merapi volcano is one of the andesitic volcanoes of the Sunda arc, which extends 3000 km from North Sumatra to the Sunda islands of East Indonesia. This subduction arc results from convergence between the Indian plate and the Asian plate (Lee and Lawver, 1995). In Java, the convergence is frontal with a speed of 6.5 cm/year (De Mets et al., 1990), although speed and direction vary along the arc (Zen, 1993). The Sunda arc is located in an area where subduction has been going on since Upper Palaeozoic (Katili, 1974). Merapi is located about 300 km from the trench and the depth of the Benioff zone is around 170 km (Hutchison, 1976).

The history of the Merapi volcano is rather complex (Berthommier, 1990; Berthommier et al., 1990; Camus et al., 2000 – this volume; Newhall et al., 2000 – this volume). Three main divisions are seen. “Ancient Merapi” (more than 60 000–8000 years b.p.) is the basement of the edifice, made principally of various andesitic breccias. “Middle Aged Merapi” (from 8000 to 2000 years b.p.) involved alternating andesitic lava flows and breccia deposits. A Mount St. Helens-type edifice collapse (Christiansen and Peterson, 1981) probably occurred during this period (Camus et al., 2000 – this volume; Newhall et al., 2000 – this volume). “Recent Merapi” (from 2000 to 600 years b.p.) is made of three main kinds of deposits: large andesite flows, nuées ardentes deposits, and deposits from phreato-sub-plinian and

sub-plinian eruptions. Merapi volcano is at present one of the most active and dangerous volcanoes in the world. The present main threat from the volcano is the collapse of an andesite dome growing at the 3000 m high summit, in a 200 m wide horse shoe-crater open towards the southwest. Collapse of the domes produces nuées ardentes (McDonald, 1972; Young et al., 1994), such as those of the 22 November 1994 eruption (Sukhyar, 1995; Abdurachman et al., 2000 – this volume).

3. An accurate Earth tide model for Merapi volcano

3.1. Objectives

Earth tides are due to the direct gravitational effect of the Moon and the Sun, combined with the deformation of Earth they induce. In Indonesia, gravity records show that the diurnal tides have low amplitudes (theoretically zero at equator), while the semi-diurnal tides reach their maximum, i.e. 90 μGal for the main lunar tide M_2 (thus 180 μGal peak to peak) (P. Melchior, pers. commun., 1994). Simple models such as Longman's (1959) are not best suited for microgravity studies because they do not take into account the gravity effect of oceanic tides (attraction and loading effects), which may exceed 15 μGal , especially on islands. The available Earth tide data for South–East Asia are not well understood despite numerous temporary tidal gravity stations established in South–East Asia for almost 20 years. According to Melchior et al. (1995), the tidal gravity effects in South–East Asia for the principal semi-diurnal M_2 tide are modelled with a precision of only 2.5 μGal . Thus we wished to establish a tidal station close to Merapi for two tasks: to establish an accurate local Earth tide model for microgravity studies; and to address the question of whether the volcano itself can introduce a perturbation of the Earth tide model.

3.2. Data acquisition

We installed the station in November 1993 at Babadan observatory post, located 4 km from the summit (Fig. 2), and recorded more than 2 years of data at 1 min interval. The recording meter must be close enough to the volcano in order to get a valid

Table 1

Results of gravity meter dial calibrations. We compute the linear regression (York, 1966) between the records (in Hz) against the screw dial value. The result of the regression is then multiplied by the dial calibration table factor, which gives the factor a and the constant b , following the equation: calibrated sample (μGal) = $S \times (\text{uncalibrated sample (Hz)}) + b$. The RMS of the regression factor are given in brackets. The variations of the admittance factor are less than 1%. The zero method increases the stability of the calibration factor. S is different between the feedback and the non-feedback mode because the frequency of the gravity signal of the meter is different for the two modes

Date	Place of calibration	S	Regression
<i>Without zero method</i>			
17 November 1993	Babadan	379.80 (0.95)	0.999912
06 August 1994	Brussels	413.76 (1.87)	0.999795
<i>With zero method</i>			
15 September 1994	Brussels	0.006194 (2.0×10^{-5})	0.999928
19 October 1994	Babadan	0.006188 (0.5×10^{-5})	0.999989
14 February 1995	Babadan	0.006255 (1.2×10^{-5})	0.999958
21 October 1995	Babadan	0.006195 (1.7×10^{-5})	0.99988
Average (1994–1995)	Babadan	0.006213 (5.2×10^{-5})	

model for the study area, but at the same time not so close that volcanic activity disturbs the recording. Moreover, the station should be installed on an heavy pillar in a seismically quiet place and in a thermostated room (less than 1°C of temperature variation over the year). At the Babadan observatory post, the bunker built during Dutch colony for protecting observers from nuées ardentes meets these requirements.

The station records the signals of the LaCoste–Romberg D131 gravity meter (belonging to VSI), two thermometers, one barometer and one hygrometer. We also record the local rainfall signal provided by the observatory. The gravity meter is enclosed in a protective box to further reduce external temperature variations. Data are stored on a PC through an Environmental Data Acquisition System designed at the Observatoire Royal de Belgique (Beauducel, 1991; Van Ruymbeke et al., 1997). A double solar panel and two batteries supply electrical power.

The records may be divided into two periods: the first from November 1993 to July 1994 and the second from October 1994 to October 1995. In the first period, the meter did not have electrostatic feedback nulling, so that instrumental phase lags need to be corrected (Rydelek et al., 1991). Analysis of the early data showed that the station had to be improved. In August 1994, this feedback nulling was fitted to the meter. According to Van Ruymbeke (1991), it reduces the tilt effects on the gravimeter sensitivity and the

instrumental phase lags are reduced. Moreover, the loss of data due to strong earthquakes is reduced to several hours (previously several days). Before reinstalling it at Babadan in October 1994, we validated this equipment at ORB (Jousset, 1996). To improve its stability, we fastened the meter onto a large, heavy baseplate. After installation, first month of data should be interpreted carefully, because of instrument stabilisation in temperature. The resulting noise on the records then appeared to be within $0.3\text{--}0.9 \mu\text{Gal}$.

3.3. Data processing

Data processing consists of calibration and reducing the effects of external parameters (pressure, temperature,...). Calibration converts the reading first to dial turns by linear regression (York, 1966) and then to microgal by the LaCoste–Romberg calibration factor. The latter slightly varies as a function of the dial turns and is 1.12296 at Babadan for meter D131. The results (Table 1) show the net calibration factor for both acquisition periods. At Babadan, it has been determined with an average uncertainty of 0.8% with no significant variation for 1995. For comparison, the results of some calibration tests carried out at Brussels are also indicated.

Data provided by two thermometers, one inside and the other outside the protecting box, show that the diurnal temperature oscillations inside the box are reduced in amplitude to 20–30%, and for shorter term variations to 45%. The temperature variation

inside the protecting box of the meter does not exceed 0.2–0.3°C for diurnal oscillations and 1°C for annual oscillations; their influence are thus negligible (P. Melchior, pers. commun., 1994). The pressure effect was corrected following the many theoretical studies on atmospheric pressure variations (Niebauer, 1988: $-0.43 \mu\text{Gal}/\text{mbar}$; Merriam, 1992: $-0.356 \mu\text{Gal}/\text{mbar}$, Sun et al., 1995: $-0.36 \mu\text{Gal}/\text{mbar}$). We chose an average value of $-0.4 \mu\text{Gal}/\text{mbar}$. The recording barometer has an accuracy better than 20 μbar . From our pressure records, the gravity effect of pressure at Babadan can be up to 10 μGal , but not more.

As an indication of the quality of a station, Chueca et al. (1985) identified a quality factor Q , which takes into account the mean square errors in the diurnal and semi-diurnal bands, and the number of interruptions in the recording. For the period going from November 1994 to February 1995, the factor Q is 5.3 for M_2 and 11.5 for O_1 , which are good values according to Melchior (1995), compared to other temporary tidal stations world-wide.

3.4. Analysis of the records and results

The improvement of the recording conditions of the station yielded 4 months of good data for analysis (November 1994–February 1995). After calibration and the pressure reduction, the digital records were analysed by Venedikov (1966) filters and a standard tidal potential development with 505 waves (Cartwright and Tayler, 1971). Melchior (1989) described the method of analysis using the Earth model of Molodensky (1961) and indirect effects of ocean tides (Farrell, 1972; Schwiderski, 1980; Francis and Dehant, 1987; Le Provost and Lyard, 1993). The tide value at Merapi may be predicted at any given moment with an accuracy better than 1.3 μGal for all components, the worst prediction being for M_2 .

The question whether the volcano itself could introduce a perturbation of the Earth tide is addressed in the last part of this paper. The conclusion here is that the records of the Babadan station provide a local Earth tide model more than accurate enough to correct our microgravity surveys.

4. Repeated network results

Figs. 2 and 3 show the location of the measurement

points, located on concrete benchmarks from the foot of the Merapi to its summit. A higher density of points encircle the active dome. In November 1993, October 1994 and October 1995, we measured the gravity and its vertical gradient at these points (JRA, PAR, SEA, SEB, GAM, PUS, PEB, PEH, NWP, DOZ, LIL, LUL, TRI, MAR-GPS, NUR, AYI, IPO, PUN). We also measured the accurate location of twelve of these points (JRA, SEA, PUS, DOZ, LIL, LUL, TRI, MAR-GPS, NUR, AYI, IPO, PUN). Tables 2 and 3 give observed gravity and elevation data.

4.1. Gravity data acquisition and processing

Most former studies used LaCoste–Romberg G or D meters whose final accuracy is about 10–20 μGal (Rymer, 1994). In the recent years, Scintrex CG3-M meters (Hugill, 1984; Seigel et al., 1990) have been used at Masaya volcano (Metaxian, 1994; Bonvalot et al., 1995), at Piton de la Fournaise (Bonvalot et al., 1996), at Etna (Budetta and Carbonne, 1997) and at Hokkaido volcanoes (Jousset et al., 1997). For all the surveys at Merapi, we used the Scintrex CG3-M gravity meter capable of measuring small gravity differences with a repeatability of about 5 μGal (Jousset et al., 1995).

Completing the measurements (gravity and its vertical gradient) at all the points of this large-range network (difference of gravity between extreme points around 420 mGal) requires four full days, over which time we assume that volcano activity does not change the gravity field. One full day is devoted to measuring the points of the profile (JRA, PAR, SEB, SEA, GAM, PUS, PEB, PEH, NWP and PUN) using a go-and-back loop (profile method, Watermann, 1957), for drift reduction. Two to three overnights at the summit area are required for completing measurements at summit stations (PUN, DOZ, LIL, LUL, TRI, MAR-GPS, NUR, AYI, IPO). Moreover, while climbing and/or going down we measured gravity vertical gradients. Our technique for measuring the vertical gradient consists of measuring gravity on the ground and on a tripod one meter above the ground (Jousset et al., 1995). Finally, each point is occupied at least three times with the exception of JRA, PAR and SEB in 1995.

We used the calibration factor obtained from the calibration line of Sèvres (Becker et al., 1995) after

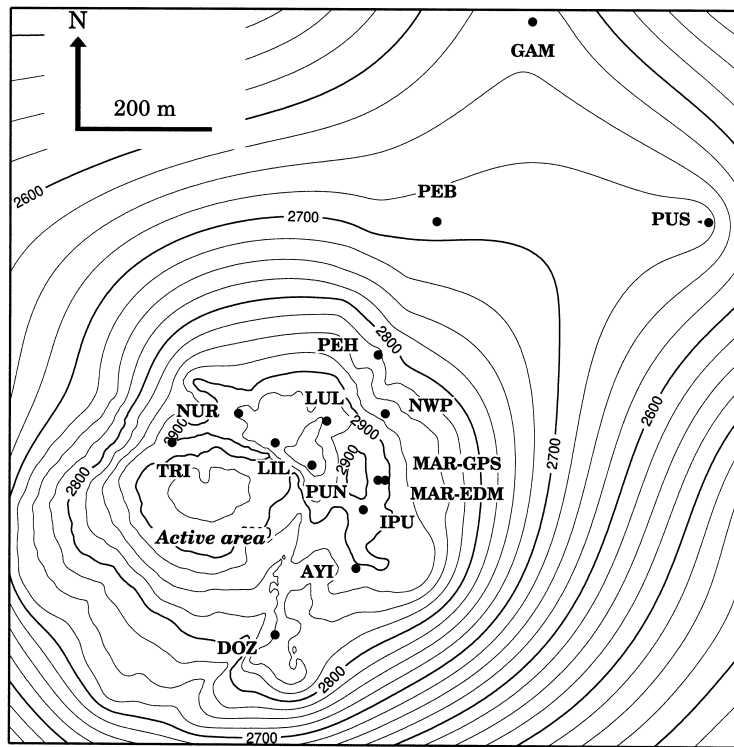


Fig. 3. Location of the points at the summit area. Note that there are more points around the active area. Values give elevation changes, above 1993–1994, below 1994–1995.

validation in Indonesia. Yokoyama and Hidikusumo (1969) and Dvorak et al. (1982, unpublished data) measured the gravity difference (about 330 mGal) between two points of the Indonesian gravity network (Ambarukmo Hotel and MVO) and two points located at the foot of the volcano (Babadan and JRA). We measured in 1994 the gravity at these points with the Scintrex meter in a further loop to get a “Indonesian” calibration factor. The difference between the Sèvres and Indonesian calibration factors is less than 10^{-5} .

After the reduction for Earth tides (given by our new local model), the reduction for the instrumental drift was carried out. The drift is a complex function, which is at the first order linear with time and also depending on temperature for Scintrex meter (Naozaki et al., 1990). The Scintrex meter allows gravity data to be compensated for the temperature change measured very close to the gravity sensor (Hugill, 1984), but this compensation is imperfect (Naozaki et al., 1990; Jousset et al., 1995). In further

controlled laboratory studies, with a room where temperature change is less than 0.1°C , tests showed that the temperature compensation of the meter strongly depends on the room’s pressure with a linear admittance value of about -4.5×10^{-4} K/bar (Jousset, 1996). This effect is not negligible on Merapi, because of the large range in the altitude of the network (about 1400 m). With a standard atmospheric model (Merriam, 1992), this corresponds to about 280 mbar.

Using the go-and-back method (or “profile method”, Watermann, 1957) and in order to remove simultaneously the time and temperature effects, we used a bilinear regression of the gravity data against time and temperature compensation value. This procedure improves the standard deviation of the results by a factor of about 1.5, compared with the single regression against time only.

The final standard error (RMS) is about 15–20 μGal for most of the points of the network, except

Table 2

Gravity data in 1993, 1994 and 1995. Reference is taken at SEA. First column gives the name of the point. For each year, the first column gives relative gravity (mGal) and second column standard error, ste (mGal)

Point	Gravity 93 (mGal)	ste (mGal)	Gravity 94 (mGal)	ste (mGal)	Gravity 95 (mGal)	ste (mGal)
JRA	294.756	0.017	294.740	0.008	294.628	0.090
PAR	192.131	0.010	192.089	0.010	191.844	0.127
SEB	61.900	0.025	61.851	0.018	61.902	0.042
SEA	0.000	0.001	0.000	0.014	0.000	0.015
GAM	-33.516	0.004	-33.493	0.005	-33.527	0.018
PEB	-43.981	0.021	-44.051	0.006	-44.011	0.011
PEH	-81.490	0.012	-81.557	0.002	-81.526	0.007
PUS	-43.616	0.001	-43.605	0.001	-43.468?	0.016
NWP			-100.093	0.002	-100.123	0.024
PUN	-127.894	0.005	-127.700	0.007	-127.863	0.010
LIL	-121.832	0.006	-121.671	0.027	-121.841	0.014
NUR	-115.380	0.004	-115.265	0.001	-115.410	0.020
TRI	-108.297	0.011	-108.186	0.025	-108.333	0.020
LUL	-123.824	0.006	-123.709	0.034	-123.858	0.012
MAG	-113.544	0.010	-113.447	0.001	-113.549	0.004
MAE	-112.651	0.011	-112.528	0.002	-112.685	0.011
IPU	-113.227	0.005	-113.110	0.003	-113.243	0.004
AIY			-106.088	0.002	-106.232	0.004
DOZ	-97.414	0.005	-97.022	0.005	-97.288	0.009

Table 3

Elevation data in 1993, 1994 and 1995. Reference is taken at SEA. First column gives the name of the point. For each year, the first column gives elevation (m) of the point and second column, standard deviation (m)

Point	Elev. 93 (m)	std (m)	Elev. 94 (m)	std (m)	Elev. 95 (m)	std (m)
JRA			1335.426	0.003	1335.548	0.033
PAR						
SEB						
SEA	2570.413	< 0.01	2570.413	< 0.01	2570.413	< 0.01
GAM						
PEB						
PEH						
PUS	2734.017	0.01	2734.014	0.003	2734.060?	0.003
NWP						
PUN	2986.723	0.009	2986.754	0.004	2986.702	0.012
LIL	2971.492	0.009	2971.506	0.005	2971.476	0.012
NUR	2953.162	0.009	2953.202	0.005	2953.180	0.012
TRI	2927.375	0.009	2927.426	0.005	2927.478	0.013
LUL	2976.776	0.009	2976.792	0.004	2976.758	0.011
MAG	2949.909	0.009	2949.925	0.006	2949.933	0.012
MAE						
IPU	2949.648	0.009	2949.677	0.007	2949.684	0.012
AIY			2927.851	0.004	2927.864	0.012
DOZ	2893.799	0.009	2983.742	0.004	2893.754	0.013

in 1995 at JRA, PAR and SEB, where only two repetition measurements were done, with more than 3 days of interval.

4.2. Elevation data acquisition and processing

Studies for which only gravity measurements are carried out are of limited use. Independent deformation data are also required, especially elevation changes. Unless the horizontal displacement is very large, as at Usu volcano in 1977 (Yokoyama, 1989), gravity variations due to horizontal displacement are negligible because the horizontal gradient of the Bouguer anomaly is small (less than $10 \mu\text{Gal/m}$ in the surroundings of Merapi). With the accuracy of gravity available (more than $10 \mu\text{Gal}$) and from the measured vertical gradient values (about $-500 \mu\text{Gal/m}$ at the summit points), the accuracy needed to correct elevation variations is about 2 cm. We used the Global Positioning System, which has the advantage for volcanic studies of needing no visibility between observation points, and of being able to operate under any weather condition. The basic principle of differential GPS is to measure the distance between all satellites in view (four at least), with the receiver antennas installed above a minimum of two of the benchmarks.

The Merapi GPS network consists of 12 benchmarks set up by Voight (pers. comm.) between 1988 and 1992 for EDM geodetic monitoring. Our team measured this network in September 1993 with two SERCEL receivers (single-frequency), in September 1994 with three ASHTECH receivers (dual-frequency) and in September 1995 with two SERCEL receivers. Data were first converted to a single RINEX format, then processed with BERNESE software (Rothacher et al., 1993). The absolute positions of network points are resolved by adjusting all vectors in space and fixing them to a known reference point. We used the AG3D program (Ruegg and Bougault, 1992), which resolves the overdetermined equation system by the least square generalised method (Tarrantola and Valette, 1982). In order to reduce possible errors due to mislocation of the antenna phase-centre with respect to the benchmark, points are measured several times by permutation of the baselines. Summit point baselines (less than 500 m long) were measured

for only 1 h, but at least 3 h were necessary for PUS, SEA and JRA baselines.

Because the baselines do not exceed a few kilometres, it is possible to use single-frequency receivers that do not correct ionospheric effects. Even for the 1994 data set (ASHTECH), we did not use the second frequency L2 in baseline computations. However, for elevation differences larger than hundreds of meters, tropospheric effects have to be corrected, at least with a simple meteorological model. For 1993 and 1994 sessions, the theoretical meteorological model included in the BERNESE program was applied; for 1995, we used a model based on recorded meteorological data (pressure, wet and dry temperature) from the Krakah post.

Final error estimations (standard deviation) are almost homogeneously distributed on all the network points, with an average of about 5 mm East, 7 mm North and 15 mm in elevation. The 1994 errors are smaller than 1993 and 1995 ones because of the use of three receivers simultaneously, thus a best redundancy of baselines in the adjustment processing. In this paper, we present only vertical deformations applied for elevation gravity estimation, with the ellipsoidal errors projected on a South–North vertical plan (Fig. 4).

4.3. Results

Technical problems during the GPS data acquisition in 1993 at JRA forced us to choose the above point SEA as the reference station for deformation. This station is well up on the mountain, preventing us to interpret any large-scale change. To get consistency with deformation data, we also choose the gravity reference at SEA.

There are small displacements (a few cm) within 1993–1995 period (Fig. 4). Largest displacement occurred at DOZ in 1993–1994 period (-5 cm). Comparable displacements are shown in 1993–1994 for IPU, PUN, TRI, NUR. In 1993–1994, the pattern of DOZ is opposite to those of other points. The pattern of PUN, LIL, NUR and to a lesser extent LUL, are similar, up in 1993–1994 period and down in 1994–1995 period. TRI exhibit a different pattern: up for both 1993–1994 and 1994–1995 periods. In 1994–1995, the pattern of LUL, LIL, NUR is similar to PUN pattern, with a smaller displacement, 3 cm.

Significant gravity changes were recorded (Table 2 and Fig. 5). At the summit area, an increase occurred in 1993–1994 (up to 370 μGal) and a decrease (up to $-270 \mu\text{Gal}$) occurred in 1994–1995. At the lower points PAR, SEB and with a less extend JRA, a small decrease of about 20–50 μGal occurred in 1993–1994. At these lower points, the variations in 1994–1995 are not well constrained due to the poor accuracy of measurements in 1995.

4.4. Reducing gravity changes

Observed gravity changes (Table 2) can be explained by the terms of Eq. (1)

4.4.1. $\Delta g_{\text{Topography change}}$: the attraction effect due to changes of the topography in the neighbourhood of the gravity stations

This occurred mainly at the summit area, where dome extrusion occurred between 1993 and 1994 and partial dome collapse occurred 3 weeks after the 1994 measurements, followed by partial resumption of dome extrusion through 1995. We computed the gravitational attraction of the topography change of the dome.

We first obtained a Digital Elevation Model with 5 m data spacing built from two unpublished (1984 and 1993) summit-area topographic maps (unknown accuracy), obtained from MVO. The accuracy of the DEM peripheral to the dome is roughly estimated from differences between the altitude given by the GPS data and the altitude of the corresponding point on the MVO map (nine points were used: TRI, NUR, LIL, LUL, PUN, MAR-GPS, IPO, AYI, DOZ). In average, the standard error of these differences is less than 5 m. We used this DEM as an approximation of the summit topography in 1993.

Then, we estimated the shape of the topographical changes between 1993 and 1994 (Fig. 6), using the basis of this DEM, photographs of the active dome (Ratdomopurbo, 1995) and ourselves and a volume of the dome of $2.6 \pm 0.3 \times 10^6 \text{ m}^3$ (Ratdomopurbo, 1995).

The change of the dome shape is much less constrained for 1994–1995 period. The eruption of 22 November 1994 (Sukhyar, 1995; Abdurachman et al., 2000 – this volume) destroyed virtually the entire 1994 dome, and was followed by renewed

dome growth. Despite the existence of the MVO topographical map for 1995, it was not possible to find a good agreement with previous maps, at areas where no topographical changes occurred. It was thus hazardous to model gravity due to the change of the dome shape for 1994–1995.

For 1993–1994 period, the gravity effect of the dome computed on the basis of these DEM (Fig. 6) and assuming a density of 2400 kg m^{-3} explains most of the observed changes in gravity with time.

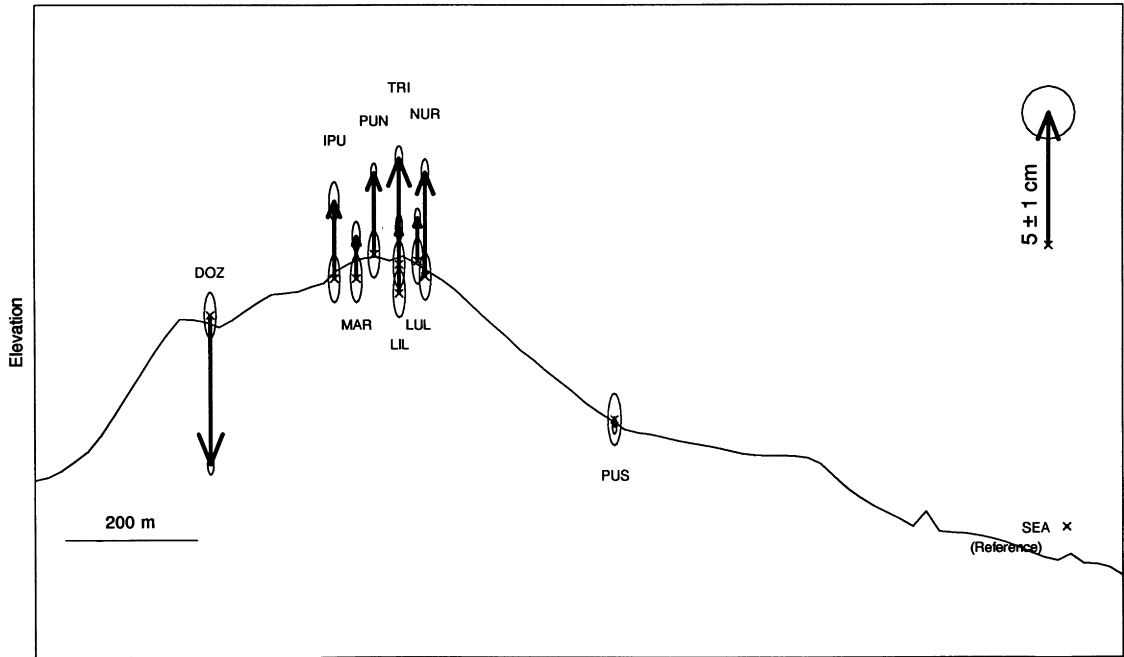
To get an idea of the uncertainties arising from the poor knowledge of the dome characteristics change (shape, volume and density), we computed for 1993–1994 the theoretical effect for different shapes, volumes and density (Fig. 5a). The uncertainties strongly depend on the location of the point, for the further the point is from the dome, the lower its gravity effect is. For dome volume and shape, two computations were carried out using the initial DEM and adding or removing 3 m at the dome elevations data. The discrepancy may rise up to $\pm 70 \mu\text{Gal}$ for the point DOZ. The effect of different dome densities ($2400 \pm 300 \text{ kg m}^{-3}$) is not large (less than $15 \mu\text{Gal}$), except for the points very close to the dome, e.g. DOZ ($\pm 50 \mu\text{Gal}$), PUN ($\pm 30 \mu\text{Gal}$). As the dome effect for DOZ is not accurately constrained, we will consider the result for this point very cautiously.

4.4.2. $\Delta g_{\text{Free-air deformation}}$: the vertical movement of the gravity station (free-air deformation)

Because the elevation changes are small, the gravitational effect of the uplift does not exceed several μGal , and thus the value of the vertical gradient is not crucial for the free-air reduction. For 5 cm of elevation change at the summit, the difference between the results obtained by using the theoretical gradient or the measured one is less than $10 \mu\text{Gal}$.

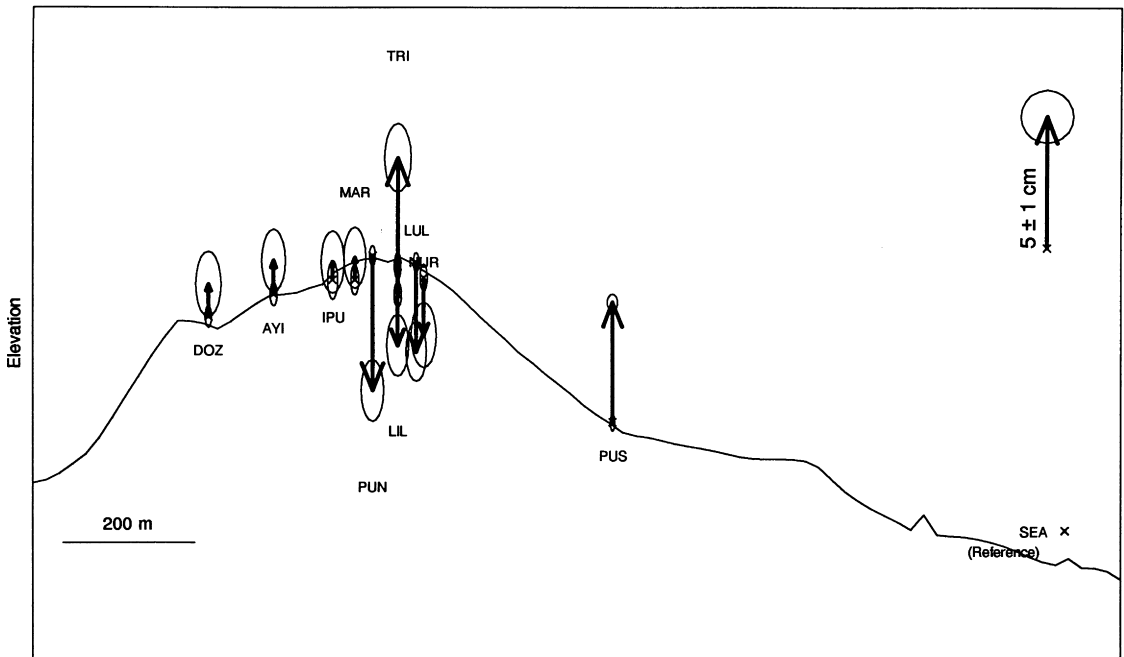
However, after reducing the large and poorly constrained dome attraction and the small and accurate elevation free-air effect, a significant signal is still present at the summit area (Fig. 7). We define this signal as the residual gravity variations (gravity variations corrected for dome attraction and elevation change effect). For this period, the largest residual gravity change (Fig. 7a) and the largest elevation change (Fig. 7b) occurred on the north-western part of the summit. A positive

MERAPI GPS VERTICAL DISPLACEMENTS SEP 1993 - SEP 1994



(a)

MERAPI GPS VERTICAL DISPLACEMENTS SEP 1994 - SEP 1995



(b)

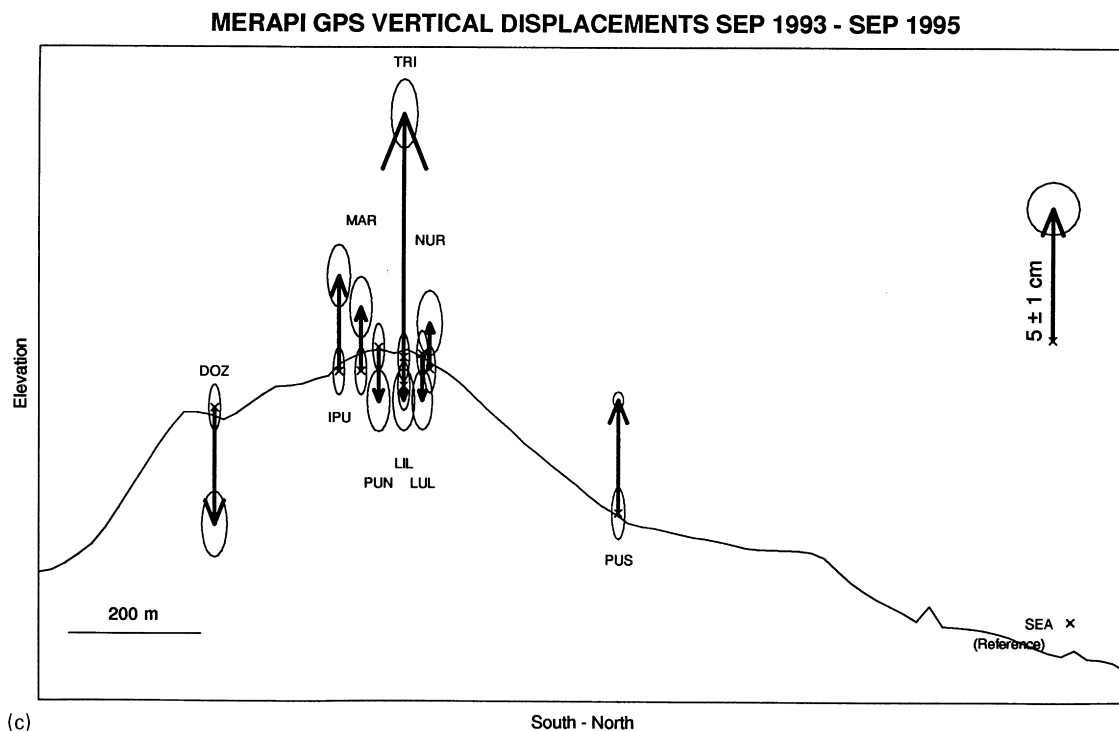


Fig. 4. Elevation changes from GPS data for 1993–1994, 1994–1995 and 1993–1995 periods in (a), (b) and (c), respectively. Small deformation occurred within these periods despite the extrusion of a dome of $2.4 \times 10^6 \text{ m}^3$ and its collapse on 22 November 1994.

correlation exists between areas of gravity and elevation changes.

4.4.3. $\Delta g_{\text{Volume change}}$: the change of volcano edifice volume, excluding “external” domes effect and free-air deformation

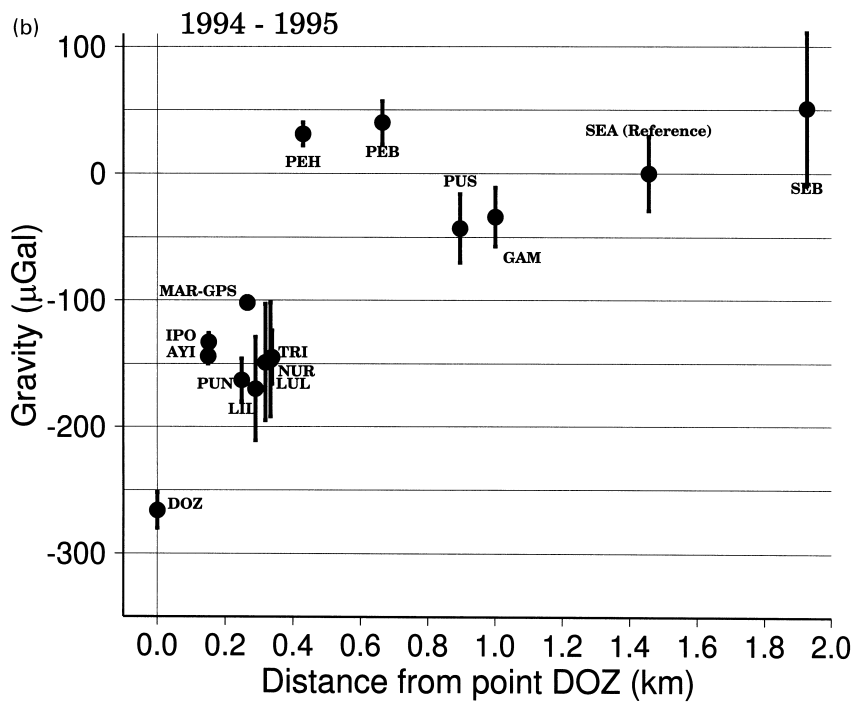
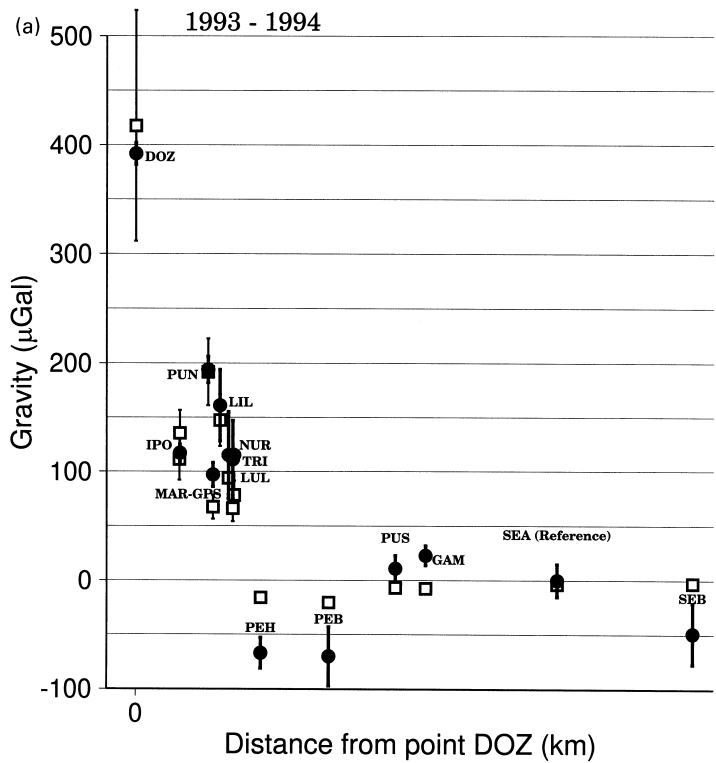
The change of volume of Merapi involves a superposition of inflation/deflation displacements due to internal processes, and a depression of the edifice due to the weight of the extruded dome. As usually done in this kind of studies (Rymer, 1994), the gravity effect of the volume change may be evaluated either by the Bouguer model, for which the volume is represented as an infinite horizontal plate of thickness the value of the elevation change (e.g. Rymer, 1994), or the Mogi (1958) model, for which the volume variation is due to an inflating/deflating spherical point in an halfspace elastic medium (Hagiwara, 1977a; Dzurisin et al., 1984; Ishihara, 1990; Wong and Walsh, 1991). Because the shape of the volcano is

neither a plate or a half-space, these modelling overestimates the effect; as the volume change is small, no matter which of these models is chosen, the local change in gravity is found to be proportional to the local elevation change. The plot of the residual gravity variations (corrected for external dome gravitational attraction and free-air deformation) versus the elevation change should be linear (Eggers, 1987).

Our residual gravity variations for 1993–1994 period versus elevation change is effectively linear as shown in Fig. 8. The gradient $\Delta g/\Delta h = 1200 \pm \mu\text{Gal}/\text{m}$ is much larger than inferred from Bouguer and Mogi theories. We hence conclude that some internal effect must be invoked. Our gradient $\Delta g/\Delta h$ is also smaller than reported for Long Valley: $6400 \mu\text{Gal}/\text{m}$ (Jachens and Roberts, 1985) and Kilauea: $29\,000 \mu\text{Gal}/\text{m}$ (Johnson, 1987).

4.5. Discussion for the 1993–1994 period

We now discuss $\Delta g_{\text{Density change}}$, the gravity effect due



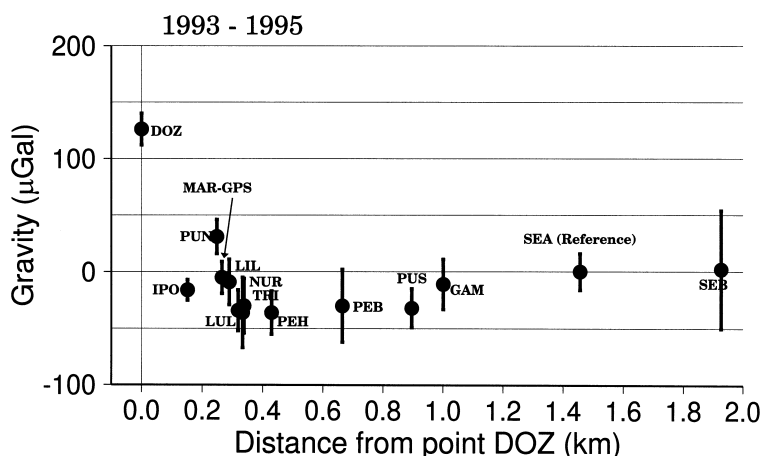


Fig. 5. Observed gravity variations for 1993–1994, 1994–1995, and 1993–1995 periods in (a), (b) and (c), respectively. Despite the small deformation (Fig. 4), large gravity variations occurred at the summit area, whereas no changes occurred far from the volcano summit. This effect is mainly due to the dome activity (see text). Error bars reflect the standard deviation of measured gravity data. In (a), the open squares indicate the theoretical attraction of the extruded dome, computed from the estimations shown in Fig. 6 and using a density of 2400 kg/m³. The error bars associated to these squares reflect the range of the possible theoretical attractions computed from different cases of domes, including shape, volume and density.

to the change of global mass inside the edifice. We estimated the net mass influx into the edifice ΔM from the surface integral of the gravity change Δg (Fig. 7a):

$$\Delta M = \frac{1}{2\pi G} \iint_S \Delta g \, dS \quad (2)$$

The results imply that the Merapi increased its mass by about 4×10^8 kg between 1993 and 1994. This value is very rough, because of the small size of the network at the summit, compared to the (largely unconstrained) contoured area. However, possibly the order of magnitude is correct, apparently closer to 4×10^8 kg than to 0.4×10^8 kg or 40×10^8 kg. Several processes may explain this apparent mass increase: (1) rise in the summit water table; or (2) magmatic processes.

4.5.1. Water level change

If due only to water, the mass increase implies a volume on the order of 0.3×10^6 m³ of pure water, distributed in the cracks and pores of the surrounding rocks. This could be represented by a few meters of water, distributed as water level change. We believe that a rise in the water table is not responsible for the gravity increase for at least three reasons. First, the repetitions of the network were all carried out before

the rainy season (from November/December to April/May). Second, using rain gauge data from the flank observatories around Merapi and assuming that summit rain fall was at least as large (3 m for the period), we estimate an annual rain water volume of about 10^6 m³ falling over the summit catchment area of about 3×10^5 m². Explaining the gravity change as a water table effect would mean that on the order of a third of the total rain fall (not just the difference 1993–1994) would have to be stored in a reservoir at the summit, which is not probable. Third, as the topography is steep and the volcano is hot (superficial temperature may exceed 830°C in the fumarolic areas and the temperature at 30–50 cm depth is generally more than 50°C), most of the summit rain should either run off or evaporate soon after it falls.

4.5.2. Magmatic processes

We address two questions: (a) what could be magmatic processes leading to apparent mass increase? (b) could the involved processes explain the dome growth?

(a) Before the material of the dome was extruded, it occupied a certain volume within the edifice. Once extruded, this volume must have replaced by void space or by new material rising from depth. The first

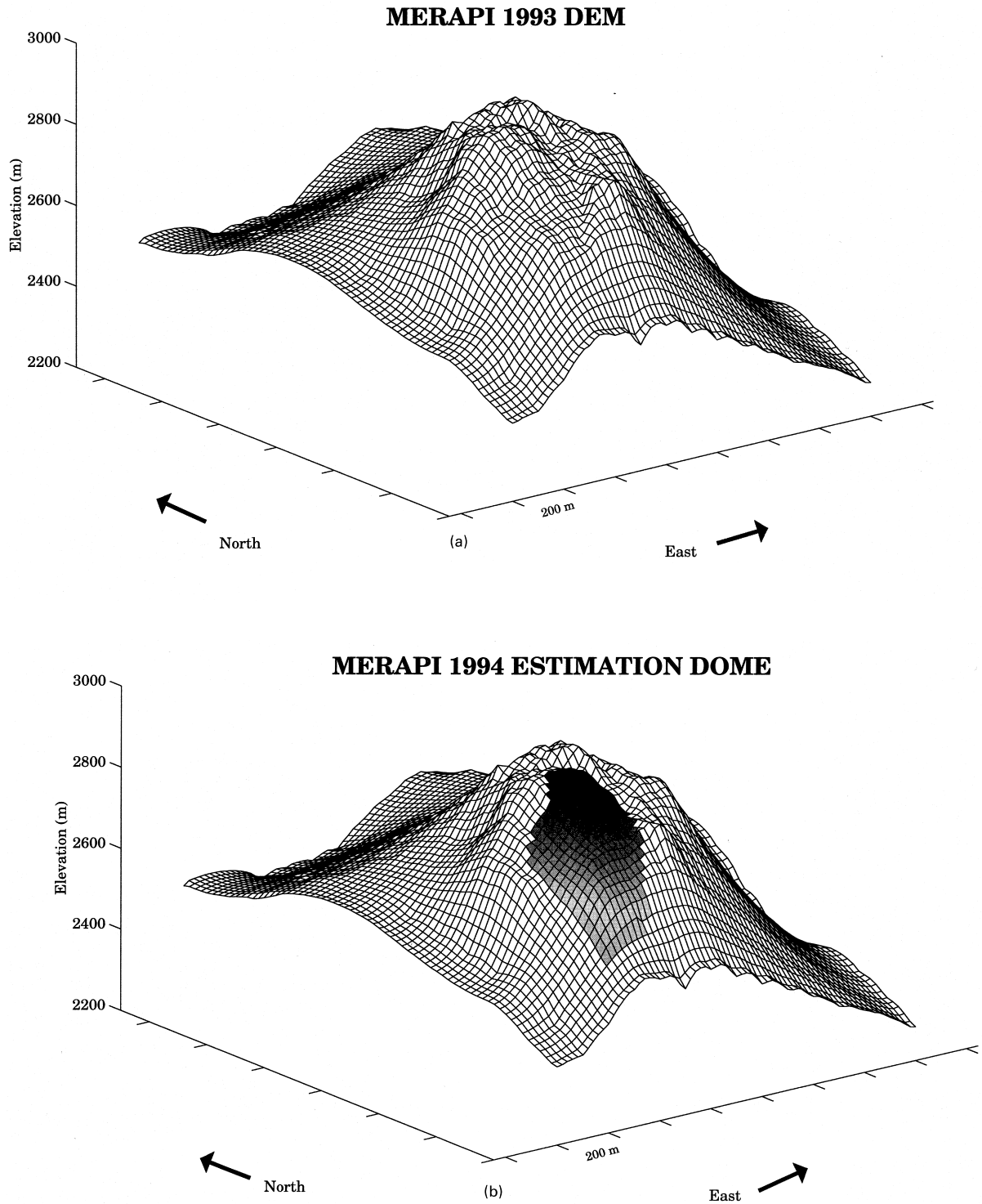


Fig. 6. 3D evolution of the dome for 1993–1994 deduced from the maps and photographs of the summit (see text). In (b), the grey shading represents the estimated dome.

hypothesis leads to a gravity decrease and probably, also deflation of the volcano; both contradict our data. Transfer of magma may occur without seismicity (Rymer et al., 1993); at Merapi, only one significant earthquake is reported which may be linked to this process, a volcano-tectonic event, type B (Voight et al., 1995; Ratdomopurbo and Poupinet, 1995). Hence, new magma probably rose at depth because gravity (corrected for dome attraction) did not decrease when the dome was extruded.

Density changes may be within a range of 50–200 kg/m³ (Williams and McBirney, 1979); taking the value of 100 kg/m³ the calculated increase of mass at Merapi corresponds to a volume of the order of $\Delta V = 4 \times 10^6 \text{ m}^3$; this volume is comparable to the volume of the dome. In order to obtain the depth of the source that could produce the observed residual gravity signal at surface, we compute for different depths the gravity field produced by either a sphere or a cylinder. The radius of the corresponding sphere, constrained by the mass increase, is about 100 m. The depth of the centre of mass of the sphere, for which the theoretical computation of the gravity effect at surface fits the data well is about 500–600 m. With a vertical cylinder of different radii (25–50 m), the centre-of-mass depth is less than 1000 m. Given the gross uncertainties of this modelling, these results are consistent with the depths of the roof of the magma chamber according to seismic data (Ratdomopurbo, 1995; Ratdomopurbo and Poupinet, 2000 – this volume) or above.

Replacement of mass extruded is not sufficient to explain the extra mass required for increasing gravity. Possibilities for explaining the extra-mass include adding magma of high density, magma intrusion volume into chamber in excess of volume extruded to surface (expansion of magma chamber) or crystallisation.

New magma could be of higher density. This question is important because it is related to the mixing of magma, which can produce very explosive associated eruptions (e.g. Pinatubo). Density is a complex function of both the temperature and composition of the magma and varies when crystallisation occurs, mostly because of the change of phase. Merapi is characterised by high temperature fumarolic zones (up to 830°C) from which degassing occurs. Gas analysis reveals that their composition has been stable for

years (Allard et al., 1995). The gas temperature, monitored monthly by the MVO staff (Yustinus, 1995, pers. comm.), remained approximately constant at the surface over the 1993–1994 period. The analysis of the lava of Merapi shows variations in the past (Bahar, 1984) but petrological observations reveal that the glass composition of the recent domes (1992 and 1994) is constant (Hammer and Cashmann, 1995; Hammer et al., 2000 – this volume). Hence, we discard the hypothesis of an intrusion of magma with higher density.

Crystallisation in a magma chamber is accompanied by crystal contraction and the release of gas species, depending on the amount of crystallisation (Tait et al., 1989). In a closed system, crystallisation would not change the mass, but with a system partially open as at Merapi, outgassing reduces the mass. At Merapi, as little deformation occurred, we assume that the chamber was volume constant. New inflow of magma may have exactly balanced volume loss due to contraction of crystals and degassing. This mass would come from depth and rise together with the steady-flow magma. The higher density of the crystallised magma would explain the increase of gravity.

(b) As a magmatic process is involved, it should be able to explain the growth of the dome. Two main processes could have triggered the dome extrusion. First, the eruption could be triggered by a magma added to the chamber from a deeper level within the volcanic system (Blake, 1984). The input of new magma causes compression of the existing liquid in the chamber, and the extrusion results, provided that the system is open. Another triggering process is crystallisation of the magma causing it to become saturated with respect to the volatile species, leading to the formation of gas bubbles and hence to a volumetric change and extrusion (Burnham, 1979; Tait et al., 1989). For Merapi, both processes could simultaneously occur (Ratdomopurbo and Poupinet, 1995).

Could the dome extrusion be a result of crystallisation? Crystallisation may create either under-pressure or over-pressure within the magma chamber (Tait et al., 1989), depending on the relative importance of crystals contraction and of release of gas. At Merapi, the gas discharge reflects the underground degassing of non-erupted magma (Allard et al., 1995). Textural analyses of Merapi lavas indicates

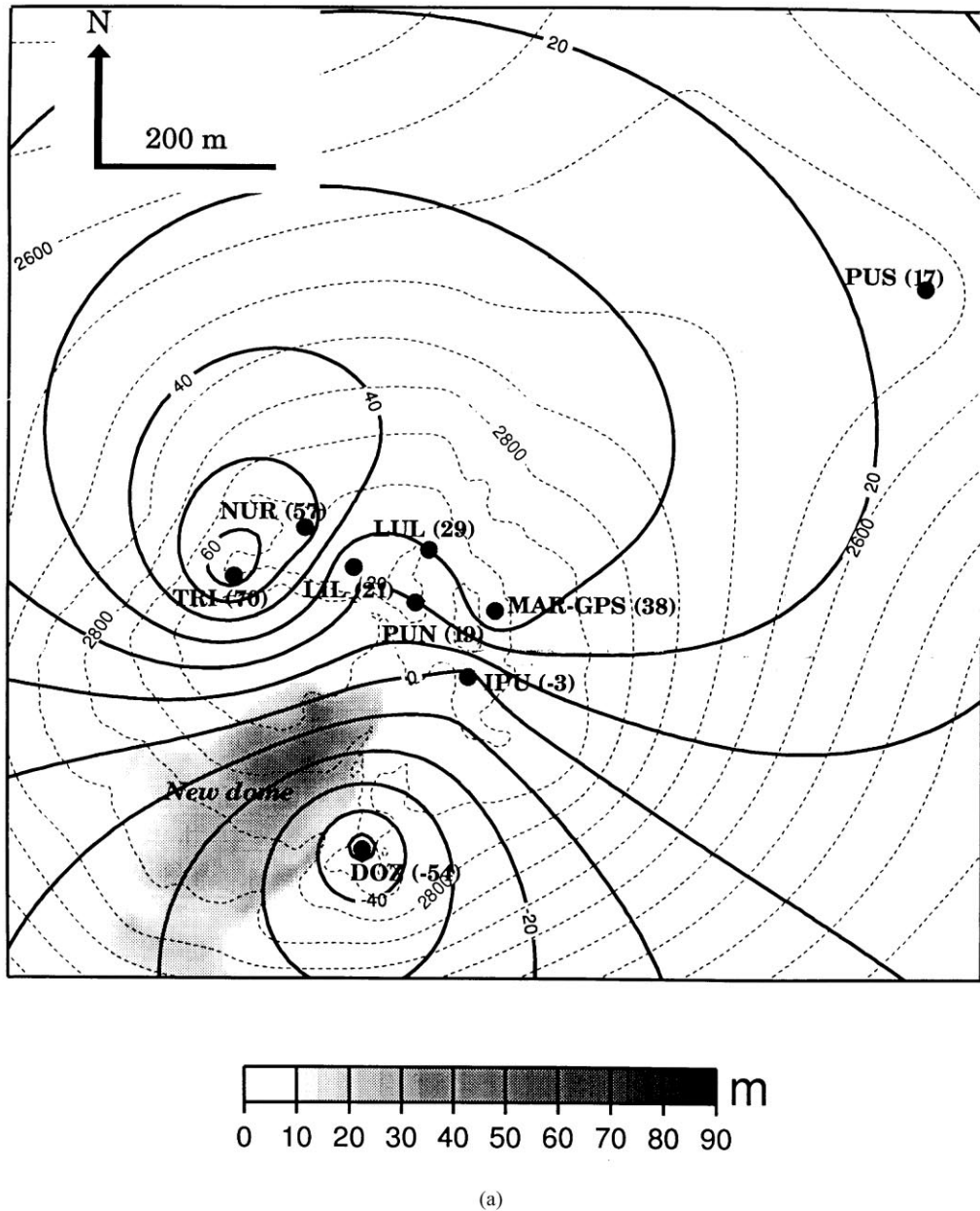
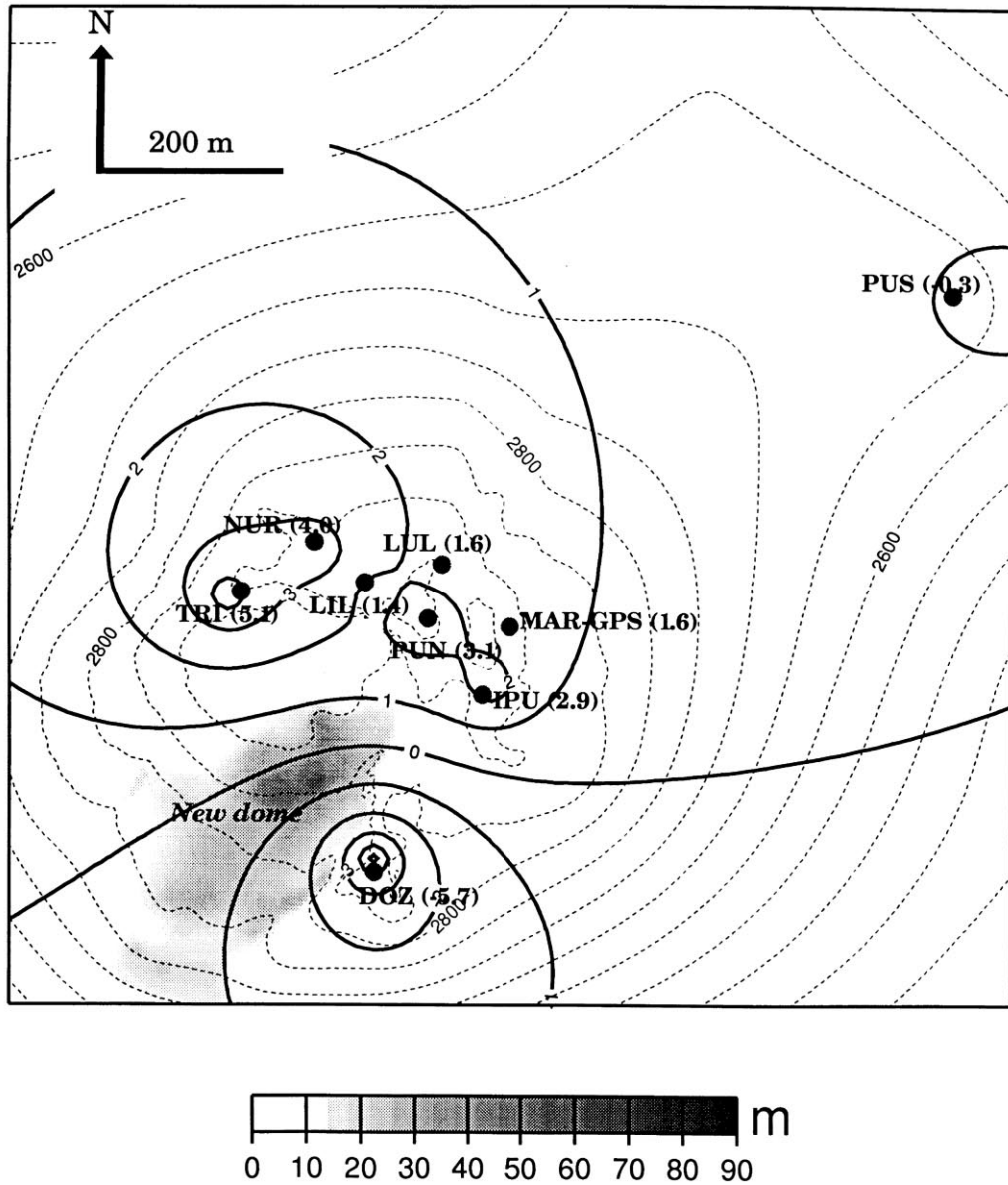


Fig. 7. Map of changes of residual gravity (a) and elevation (b) variations within 1993–1994. Values of the changes are indicated in brackets. The topography contours are dashed lines. Grey area corresponds to the thickness of the new dome and rock falls approximately. Density of 2400 kg/m^3 is assumed; in (a), solid lines represent the residual gravity variations (μGal); in (b), solid lines represent the elevation variations (cm). The north–west side of the summit is characterised by uplift and gravity increase. Computation of contours were made using the command “surface” of GMT 3.0 (Smith and Wessel, 1990), with a tension factor of 0.75 for (a) and 0.25 for (b).



(b)

Fig. 7. (continued)

rapid nucleation and growth crystallisation resulting from high supersaturation (Hammer and Cashman, 1995; Hammer et al., 2000 – this volume). Thus, the growth of crystals may have occurred with over-pressure conditions. For the end-member case in

which the magma chamber is crystallising in a closed system, we can deduce the pressure increase within the magma chamber (Tait et al., 1989) from the mass crystallised ratio (ratio of the crystals mass to the magma chamber mass). Assuming that crystallisation

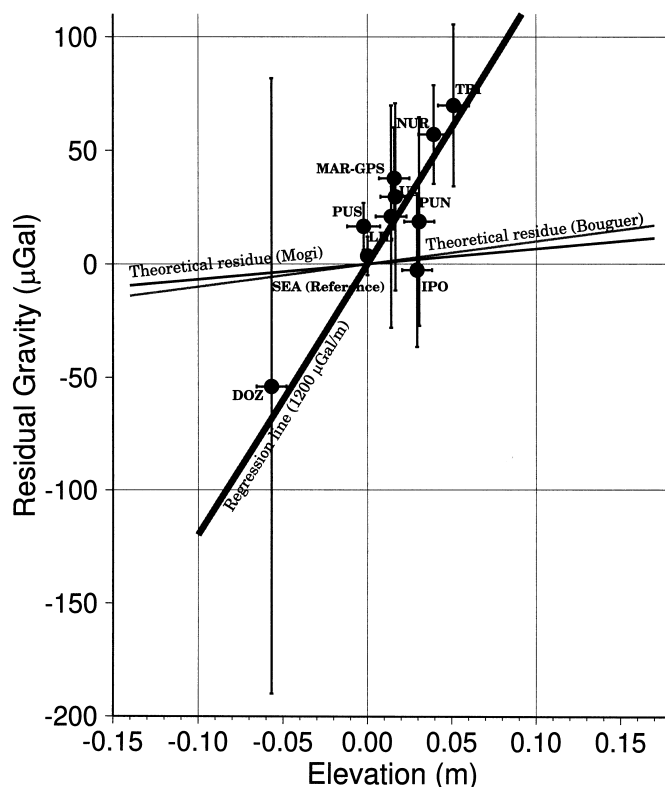


Fig. 8. Residual gravity changes versus elevation changes for the 1993–1994 period. The gravity effect of a dome volume of $2.4 \times 10^6 \text{ m}^3$ and density 2400 kg/m^3 has been taken into account. Errors bars include the uncertainty on the dome volume, shape and density. If no volcanic effect was involved, the observed residuals should follow the Mogi or Bouguer lines. Since this is not the case, this plot shows that a mass and density redistribution occurred inside Merapi during the given period.

occurs in a spherical magma chamber (radius 600–800 m and density $2200\text{--}2400 \text{ kg/m}^3$), the ratio of new mass (from our gravity data) to the mass of the spherical magma chamber would be less than 10^{-3} , leading to a pressure increase of about 0.2–0.4 MPa. This result is obtained assuming that the contraction due to crystallisation is small, that the initial pressure in the magma chamber is at least 50 MPa and taking an initial mass fraction of gas of $0.5\text{--}1 \times 10^{-2}$. This overpressure leads to a small volume increase of the magma chamber (less than $2 \times 10^3 \text{ m}^3$), in agreement with the small deformation observed at surface. Using this value in Eq. (23) in Tait et al. (1989), the extruded dome would be between 1 and $6 \times 10^6 \text{ m}^3$, which is the same order than the observed extruded volume. From seismology (Ratdomopurbo, 1995) and deformation monitoring (Voight et al., 1994; Young et al., 1994; Young and Voight, 1995),

the 1990–1992 period was characterised by intrusion at depth, with concomitant cooling.

Hence, a combination of steady-continued magma influx and crystallising in the magma chamber could explain the gravity change and the small vertical deformation observed at Merapi. Furthermore, the amount of new crystals consistent with gravity observations, is also consistent with overpressure required for the growth of the dome. We suggest that the mass was added within the north-western side of the edifice, increasing gravity in this area at surface.

4.6. 1994–1995 period

The analysis conducted for the 1993–1994 period is not as straight-forward for the 1994–1995 period, because the dome height and volume are not as well known as for the first period. Due to the collapse of the

dome, the accuracy of the digital elevation model is not as good as it could be. The error introduced by the poor 1995 topography knowledge is much larger than the initial gravity signal, so that the residual gravity may have no meaning.

5. Correlation between gravity and volcanic activity from continuous records at Babadan

5.1. Position of the problem

Volcanic activity can affect continuous gravity recordings in two ways:

(1) a direct gravitational effect due to mass movement or density change;

(2) an indirect effect through the change in the mechanical response of the edifice to the tidal forces.

With regard to (2), can a change of volcano structure (e.g. a rheology change due to an intrusion or a release of gas within the chamber) modify its response to the tidal forces with time? To answer this question, we must determine whether the amplitude and/or the phase of records change with time, relative to the theoretical response of the Earth. This ratio between the records and the theoretical response of the Earth, i.e. the tides, is what we call admittance. Assuming pure gravitational effect has been removed, the recorded signal depends upon: (1) the gravity meter sensitivity (a purely instrumental effect); and (2) the response of the Earth to the tidal force. We are looking for changes in the response of the Earth to tidal force, hoping that the sensitivity of the meter is constant. As the latter may vary, the admittance of the gravity meter is controlled by the combination of the response of the Earth and the sensitivity of the meter.

5.2. Analysis of the records

For determining the admittance of the meter at Babadan station (a combination of the sensitivity of the meter and the response of local ground to tidal forces), we used a linear regression of, on the one hand, the derivative of the records against, on the other hand, the derivative of the theoretical model for Earth tides, over a sample window of a short period of time, typically less than 3 days (Van Ruymbeke, pers. comm., see Appendix A). Over this short period of time, this regression gives two results: (1)

the linear drift value of the meter; and (2) the admittance of the meter at Babadan. By sliding the sample window, this method is being able to follow continuously the variation with time of the meter admittance and of the linear drift. Non-tidal effects are assessed by computing the difference of the gravity record (calibrated using the value of the admittance) and the Earth tide model. We finally get the admittance and the residual drift (non-tidal effect corrected for pressure).

For Babadan data, we analyse data of 1993–1994 period and 1994–1995 period separately, because the meter acquisition system was different for the two periods, regarding the feedback nulling (see Section 3). No data are available between June 1994 and October 1994, because we transformed the acquisition system of the gravity meter. For both periods, we obtain the variations of the meter admittance and the residual drift with time (Figs. 9–12). Data gaps reflect large earthquakes (the sensor is very unstable) or technical problems.

For each period, we normalised the admittance with its average value, so that the normalised admittance curves (Figs. 9a and 10a) oscillate around one. Before normalisation, the values of the admittance computed with the new method are consistent with the calibration values of Table 1. We calibrated the records using the average value of the admittances obtained from the sample windows regressions. After the pressure effect reduction, we removed from data an average value of the linear drifts ($8.5 \mu\text{Gal/day}$), obtained from the sample windows regression, to get the residual drift. We do not interpret this average linear drift as a volcanic effect, but as the long-term drift of the gravity meter.

In the residual drift curves, most of the short-term spikes are due to earthquakes. When the level of the residual drift changes abruptly after earthquakes (less than $30 \mu\text{Gal}$), we adjusted the curves in order to present a continuous global shape, assuming that the jumps were only due to instrumental effects.

5.3. Correlation of the results with the volcanic and seismic activity

Several types of earthquakes characterise the seismic activity of the Merapi volcano (Ratdomopurbo, 1995; Voight et al., 1995): volcano-tectonic type A

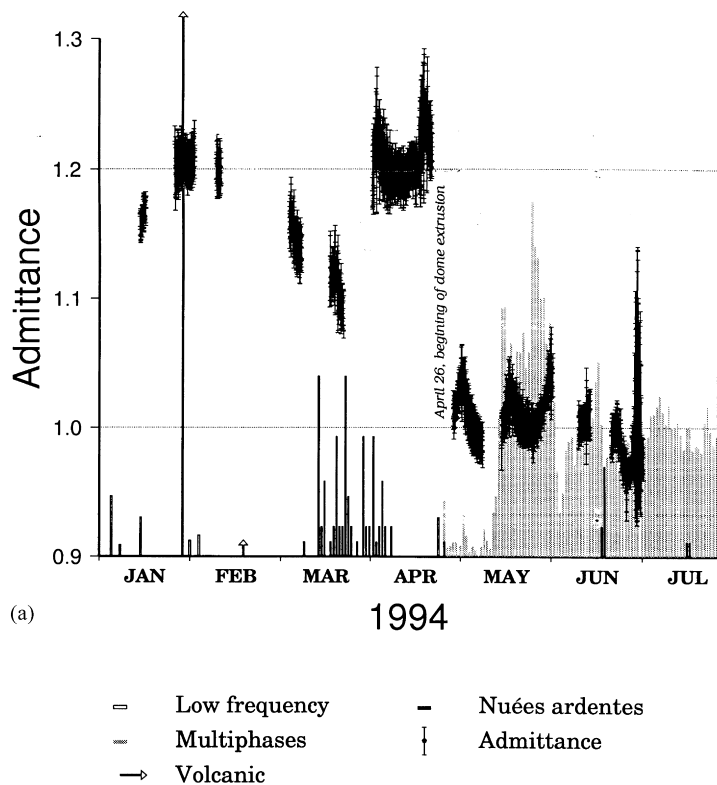


Fig. 9. Variations of the normalised meter admittance (a) and of the residual drift (b) for 1993–1994 period. The normalised admittance values are obtained by the ratio of each admittance value by the average of all admittance values. Vertical bars indicate seismic and volcanic events. In (a) a clear correlation exists between the beginning of the MP events, corresponding to the start of vigorous dome extrusion (April 26th) and the drop of the meter admittance. In (b) the minimum of the residual drift is correlated with the occurrence of the nuées ardentes of March 1994.

(VTA), earthquakes occur at depth greater than 2 km; volcano-tectonic type B (VTB), earthquakes are shallow, within a radius of 1 km around the active crater; multiphase (MP) events are superficial and occur when the dome is growing; low frequency (LF) events and tremors seem to be associated with shallow fluid movement. Moreover, nuées ardentes occur when a part of the dome collapses; their occurrence commonly indicates dome growth, which in turn suggests overpressure conditions inside the volcano (Young et al., 1994).

Comparison of both normalised admittance and residual drift variations with volcanic and seismic activity shows clear correlations, both at long term and short term (Figs. 9–12).

5.3.1. 1993–1994

The normalised admittance varies more than 20%

for 1993–1994 period (Fig. 9a), with a high level (about 1.2) from January 1994 to April 1994, with a relative lower level in March 1994. A sudden drop (almost 20%) occurs in the third week of April, corresponding to the beginning of a series of MP events. These are linked to the new phase of dome extrusion, which began on 26 April. The residual drift (Fig. 9b) shows a long decrease (about 200 μGal) until March 1994, followed by a steady large increase of about 150 μGal , and then stabilisation in June 1994. In March and April 1994, many nuées ardentes occurred, correlated with both a low and declining level of the admittance, and the minimum in the residual drift. Moreover, there appears to be a jump in the residual drift at the time nuées ardentes initiated. Both curves are stable after May 1994, correlating with no strong activity.

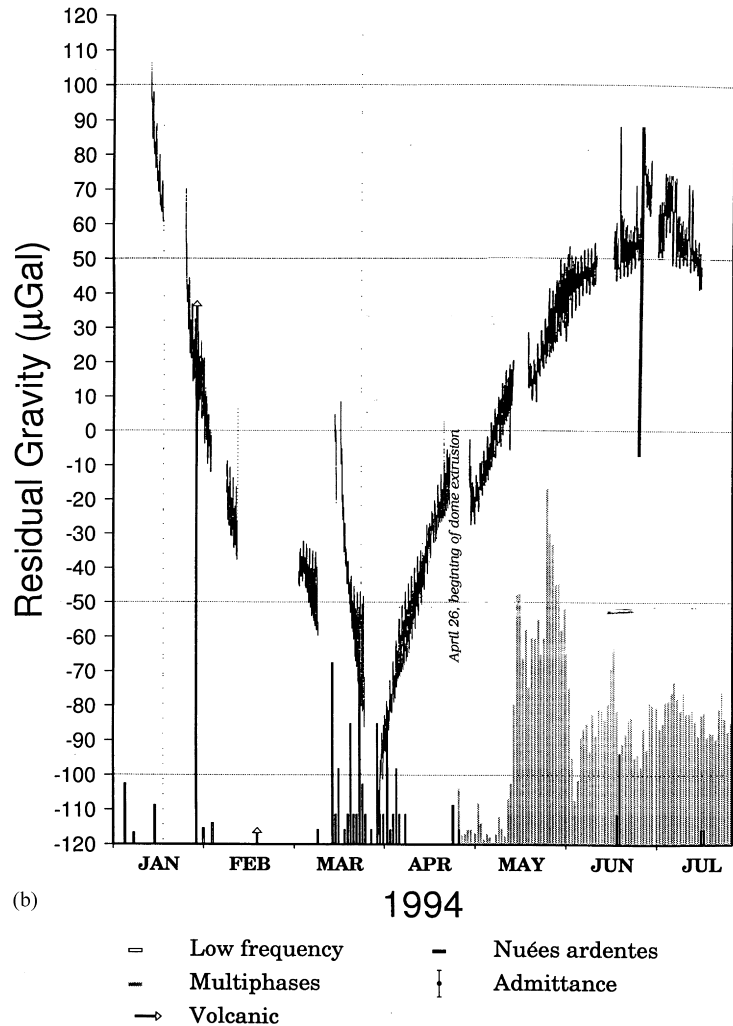


Fig. 9. (continued)

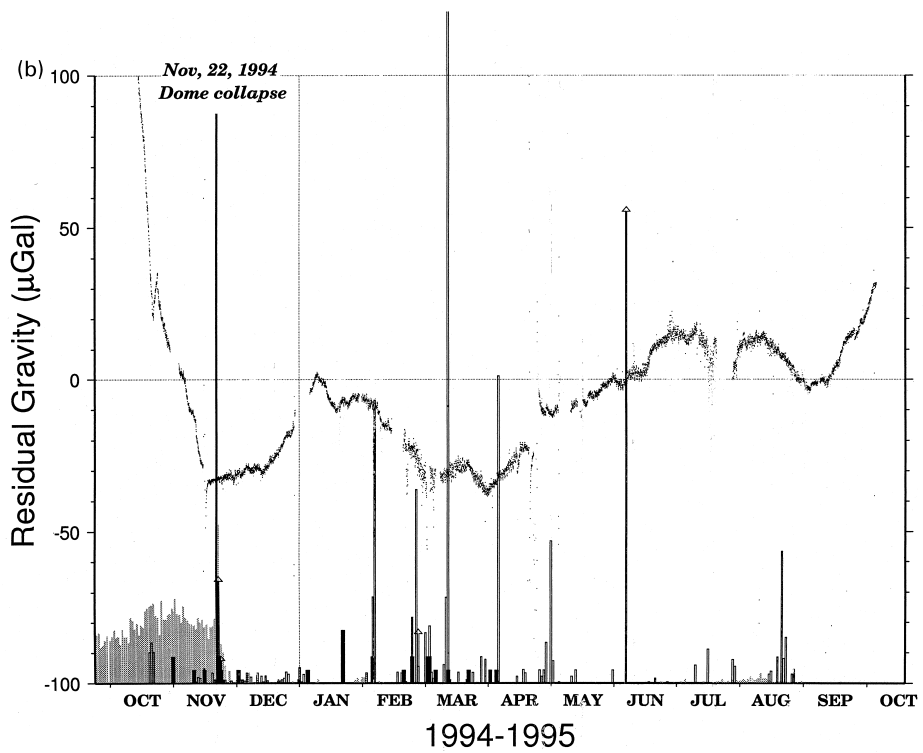
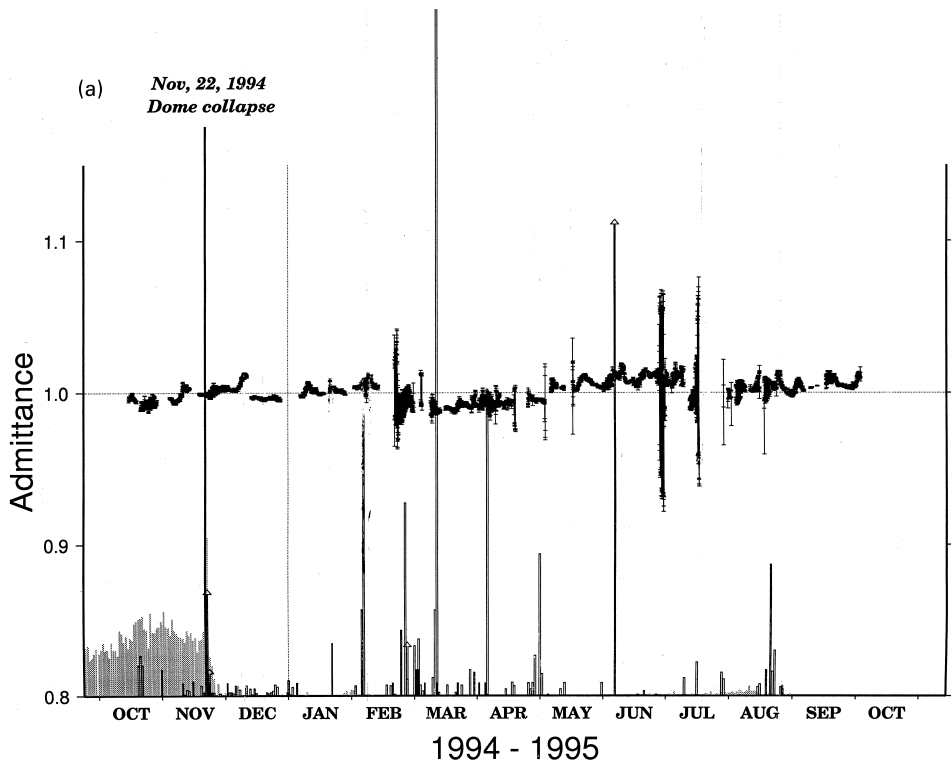
5.3.2. 1994–1995

During this period, when the station had been improved (see Section 3.2), the normalised admittance remains about one with low amplitude fluctuations of about 3% (Fig. 10a). The period for which the admittance is slightly lower than one (e.g. from mid-February to the end of April) apparently corresponds to the occurrence of LF activity, whereas when admittance >1, no strong activity is observed. In July 1995, a relative decrease of about 1.5% occurred, correlated to an increase in the seismic activity.

The residual drift (Fig. 10b) decreases until the end

of November 1994 and then exhibits oscillations (30–40 µGal) of long period (3–5 months), modulated by non-periodic variations of smaller wavelength (7–40 days) and lower amplitude (10–20 µGal). Generally, decreases of residual drift are correlated with a significant level of LF events and/or nuées ardentes (e.g. January–April 1995 or August 1995). On the other hand, the residual drift increases when few LF events and nuées ardentes occur (May–July). Residual gravity decreases sharply before the eruption of November 22, and slowly increases afterwards.

An example of a short-term correlation is shown in



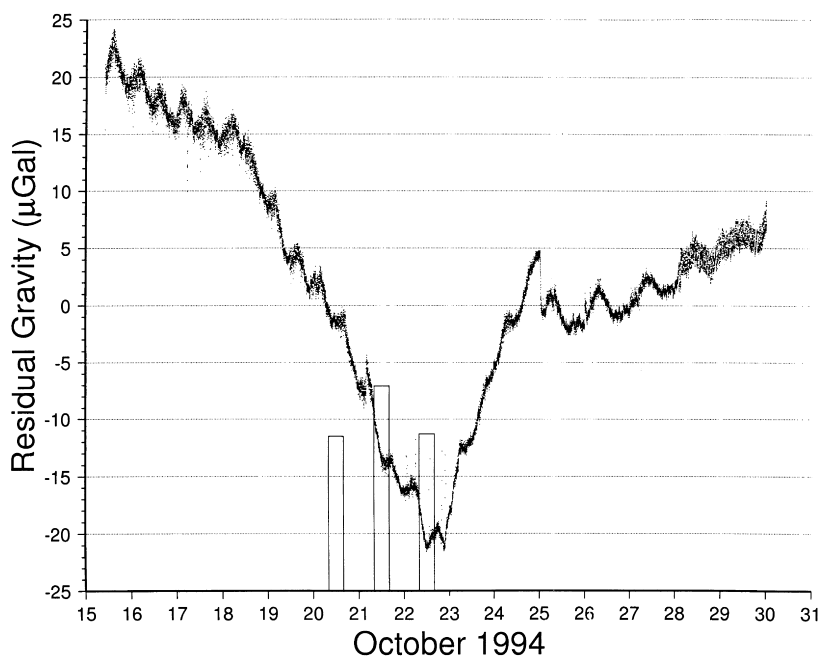


Fig. 11. Detailed residual gravity variations for several days in 1994, showing an apparent correlation between the residual drift of the meter and the LF seismicity.

Fig. 11. The residual drift decreases until the occurrence of three LF events on 20, 21 and 22 October and then increases. The dome collapse of 22 November 1994 (Fig. 12) corresponds to a change in the amplitude of the residual oscillations, from $\pm 1 \mu\text{Gal}$ before the collapse, to $\pm 2\text{--}3 \mu\text{Gal}$ afterwards. The frequency of the residual also changes with time; the residual gravity power spectrum peaks at 23–25 h for 3 days before the dome collapse, and shifts to 11–13 h afterwards. The residual drift also shows small oscillations of about $1\text{--}2 \mu\text{Gal}$, due to the poor modelling of the wave M_2 .

5.4. Interpretation and discussion

De Meyer et al. (1995) showed at Etna that humidity may have a long-term effect on gravity data, but we have not observed such an effect at Merapi. Likewise,

rainfall has apparently no correlation with residual gravity. Three hypotheses may thus be invoked: a direct gravitational effect, tilt or elevation variation effects. A direct gravitational effect should be very small, because the Babadan meter is located 4 km to the summit area (direct attraction of the dome is less than $1 \mu\text{Gal}$ at Babadan) and 3 km from magma chamber (approximately at the same elevation). We thus interpret the residual gravity variations in terms of either tilt and/or elevation change. Unfortunately, continuous data for neither elevation nor tilt are available to enable discrimination of one from the other. Long term variations of the gravity data would give an indication that Babadan either tilts or inflates by an amount of ± 50 to $150 \mu\text{rad}$ (computed from gravity variations due to instrument tilting) or 5–15 cm (computed using the measured vertical gradient of gravity at Babadan, i.e. $-279 \mu\text{Gal/m}$), respectively.

Fig. 10. Variations of the normalised admittance of the gravity meter (a) and of the residual drift (b) for 1994–1995 period. The normalised admittance values are obtained by the ratio of each admittance value by the average of all admittance values. There is a correlation between the residual gravity and seismicity.

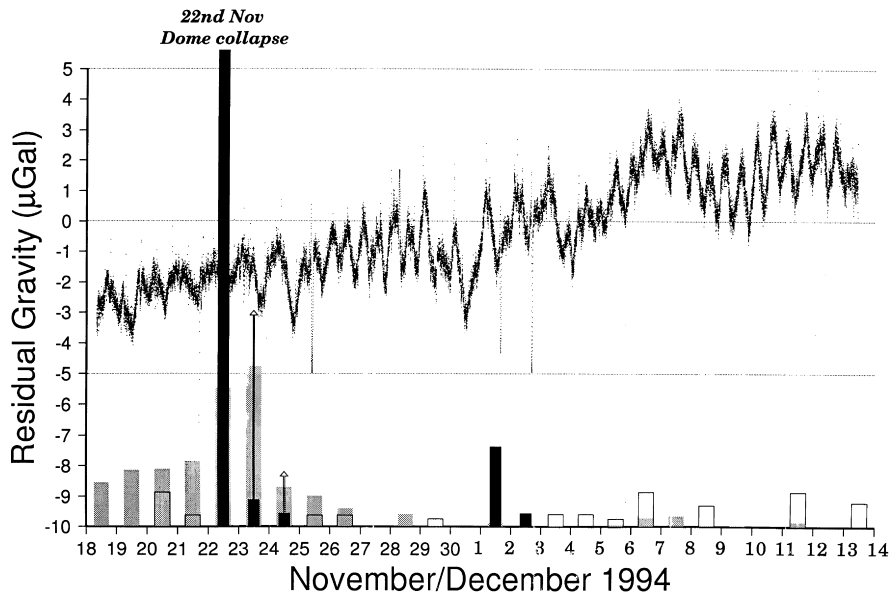


Fig. 12. Detailed residual gravity variations, showing a correlation of the change of amplitude with the 22 November 1994 eruption. Moreover, a change in the frequencies of the record can be evidenced (see text).

It is much more difficult to interpret the admittance variation, although data suggest that it is not only due to instrumental effects, because of the correlations with the volcanic activity and seismicity.

We presented above (Section 4) a crystallisation model for explaining the Merapi activity during 1993–1994. With further crystallisation, the pressure may have increased in March–April 1994, causing a decline in the residual gravity, the gas indirectly causing surface movements and nuées ardentes. Then, the pressure may have decreased, while the dome was growing. We assume that this process may have continued in 1994–1995 and suggest that the residual gravity variations are due to pressure variations within the volcano. Brandeis and Jaupart (1987) show that temperature oscillations and composition changes occur when crystallisation proceeds explaining zonal composition within minerals. Oscillatory zoning of plagioclase phenocrysts (Hammer and Cashman, 1995) could indicate oscillating pressures due to gas escape episodes and gas pressure building.

Seismological data indicate that LF events are generally related to superficial activity. They are, however, correlated to gravity variations recorded at 4 km west of

the summit. Pressure increases as residual gravity declines (Fig. 9a). Then the overpressure causes release of gas (and superheated steam). Flow of these pressurised fluids causes LF events, pressure declines and residual gravity rises, 4 km from summit.

There is no evidence from gravity data that the dome collapse of 22 November 1994 is due to an internal process. The large decrease of the residual drift may be partially due to the time for the station to stabilise, which usually takes about one month. This time is exceeded as the gravity still decreases before the eruption. Moreover, it seems to have modified the response of the volcano to the tidal potential as seen in the amplitude and frequency of the residuals and admittance.

6. Summary and conclusions

During 1993–1995, we carried out several microgravity and GPS measurements on a repetition network and we recorded the continuous gravity variations at Babadan observatory.

From repeated measurements:

- (1) We observed significant gravity variations (up

to 370 μGal), but small deformation (less than a few centimeters).

(2) A large part of the gravity signal is explained by the topographical variations due to the dome growth and collapse. However, positive residual gravity changes remain, implying that the mass of the extruded dome and of the released gas must have been at least replaced inside the volcano.

(3) In order to explain the positive residual gravity in 1993–1994, we suggest a partial crystallisation model involving earlier intruded magma (in 1990–1992) and additional material supplying in 1993–1994. The increase of pressure resulting from crystallisation, together with the buoyancy of the residual liquid is sufficient to drive further dome growth.

From the continuous records:

(4) An accurate Earth tide model for the Merapi volcano is now available, with an accuracy of 1.3 μGal for M_2 .

(5) We also show that both the residual drift and the admittance are correlated with the volcanic activity.

(6) Assuming that crystallisation continued in 1994–1995, the oscillations of the pressure release, increasing due to crystallisation and decreasing due to gas release to the surface, could explain the variations of the residual drift observed at Babadan via instrumental tilt. The correlation of the admittance with the volcanic activity is not straightforward and must be discussed further.

We also have shown that the continuous recording and the repetition network results are consistent with other data. Our results confirms that repetition networks and continuous gravity recording are promising techniques for studying and monitoring volcanoes. Finally, there may be a hope for possible forecasting of nuées ardentes, dome collapse, from the variations of the continuous gravity monitoring.

Acknowledgements

We are grateful to Dr Wimpy Tjetjep, Director of the Volcanological Survey of Indonesia and Dr J. Sukyar for equipment facilities, and transportation. We also thank Dr H. Harjono (LIPI) for his help. Topographic maps of summit were digitised from documents drawn by Pak Sadjiman (MVO), based on numerous surveys led by him. Gravity meter

(VSI) maintenance was carried out by Nurudin, Hendra, and M. Dejean. The meter was transformed to feedback zero-method by M. Van Ruymbeke. We thank Pr. Paquet (Director of the ORB) and Pr.P. Melchior for their encouragement. The tide analysis was made at Observatoire Royal de Belgique by M. Vandercoilen and B. Ducarme at the International Center for Earth Tides at Brussels. We benefited from many fruitful discussions with C. Deplus, S. Bonvalot, and M. Van Ruymbeke, all along the study. M. Van Ruymbeke also suggested the method based on the short-arc analysis. Comments of R. Hipkin led to a much-improved manuscript. We finally thank reviewers (C. Finn, R. Jachens, K. Young, and B. Voight) who greatly helped to improve the final version. This study was supported by the French Délégation aux Risques Majeurs (Ministère de l'Environnement), by the Ministère des Affaires Etrangères and the French Embassy at Jakarta. IGP contribution Number 1661.

Appendix A. Computing the admittance and the linear drift of a continuous recording meter

A.1. Method

The object of this method is to obtain the variation of the admittance (combination of instrumental sensitivity and local earth tide response) and the linear drift of the meter with time.

Calibration consists of multiplying the reading by a constant C (in $\mu\text{Gal}/\text{reading unit}$) to get calibrated data in μGal . One may calibrate the records against the accurate Earth tide model, by a linear regression between data and model:

$$Cg_{\text{record}} = g_{\text{Earth tide}} + at + b + \dots \quad (\text{A1})$$

where:

g_{record} is the uncalibrated reading (reading unit);
 $g_{\text{Earth tide}}$ the gravity effect due to Earth tide, modelled by an accurate model (μGal);
 a the linear drift of the meter ($\mu\text{Gal}/\text{time unit}$);
 t the time (time unit); and
 b the constant of the relative gravity meter.

The direct regression between two short arcs of raw

data and of the corresponding model is limited by the drift of the meter, which changes with time due to instrumental and external parameters effects (e.g. pressure). In order to remove the linear component of the drift, a regression through the derivative of both inputs (raw records and model) is more appropriate:

$$C \frac{dg_{\text{record}}}{dt} = \frac{dg_{\text{Earth tide}}}{dt} + a + \text{error} \quad (\text{A2})$$

Two main results are then obtained:

(1) The intercept of the regression line with the y -axis gives the linear drift value a , with an error containing the temporal variations of the calibration coefficient with time and the effect of the variations of the external parameters.

(2) The regression coefficient C gives the admittance for a given period. A value of $C = 1$ indicate that the meter records the theoretical gravity effect, with no phase lag.

A.2. Mathematical formulation

Let us consider a sampling window $[X(0), X(1), \dots, X(i), \dots, X(N)]$ of a record with $X(i)$ the record value at time i of the recorded parameter X and N the total number of the samples; consider the corresponding theoretical modelling for X values $[M(0), M(1), \dots, M(i), \dots, M(N)]$ with $M(i)$ the value of model M , computed at the same time i . The approximation of the derivative is based on the underlying idea of the Newton's method for finding the zeros of a function (Kreyszig, 1988). As data and model are known at discrete time, two first order finite difference series are generated by computing, simultaneously:

$$D_{\tau}(i) = X(i + \tau) - X(i) \quad (\text{A3})$$

$$T_{\tau}(i) = M(i + \tau) - M(i)$$

with: τ time difference between the two values of X and M . If divided by τ , these differences are an approximation of the derivative of X and D . The computation of the linear regression through these differences leads to the apparent admittance T_{τ}/D_{τ} between data and model for the time difference τ and the value of the apparent linear drift $a\tau$ for the duration τ .

Computing this linear regression for several values

of τ , the zero-drift admittance is obtained by the computation of the limit, for τ tending towards 0:

$$C_N = \lim(T_{\tau}/D_{\tau}) \quad (\text{A4})$$

of the apparent admittance for τ going towards 0. Computing identically the regression between the different apparent linear drift values $a\tau$ and τ itself leads to the drift a per unit of time.

By shifting the sampling window by an amount of time, it is possible to follow the meter sensitivity continuously with time.

The two parameters τ and N must be properly chosen. The regression computation must imply enough oscillations to obtain an accurate slope value and to increase the signal to noise ratio for each τ . The value of τ cannot to be too small, because the signal/noise ratio decreases with a decrease of τ . Both of them depend on the amplitude and the period of the main signal.

The value of the calibration factor is not perfectly accurate, if there is a phase lag between records and the theoretical model. The phase lag is given by the ratio between the ellipse axis lengths, by drawing the Lissajou's plot for computing the calibration factor (Jousset, 1996).

A.3. Application to Earth tides

For Earth tides the M_2 wave controls τ and N . The period of the tides being 12 h, values of τ are chosen to be from 1 h to more than the half of the period, say 8 h. We use a sampling window of length $N = 3000$ points, i.e. 2–3 days, involving 5–6 semi-diurnal and 2–3 diurnal oscillations.

Before we applied this method to the Babadan data, we tested this method using synthetic signal of the gravity field and the corresponding theoretical Earth tide (Jousset, 1996). The synthetic gravity signals are generated by the theoretical model, disturbed with a linear drift or a quadratic drift, or a sudden change of drift. Tests conducted for various values of N reveals that this parameter has no strong effect on the C_N solutions. The strongest effects arise when introducing a constant phase lag between synthetic signal and theoretical one. In such a case, the plot of the differences T versus D shows an ellipse, of which the ratio between long and short axes is a function of the phase lag.

More generally, this method may be used for computing the admittance between any input signal and a theoretical model of its variations, but also for computing the admittance between two signals. The difficulty arises when a large phase lag exists, for example the residual of the gravity variations after Earth tide correction and the pressure, because it may affect the values of the amplitude. Possible phase lags of M_2 between data and model may alter the true value of the regression coefficients.

References

- Abdurachman, E.K., Bourdier, J.L., Voight, B., 2000. Nuées ardentes of November 22 1994 at Merapi Volcano, Indonesia. *J. Volcanol. Geotherm. Res.* 100, 345–361.
- Allard, P., Carbonnelle D., Dajlevic, D., Metrich, N., Sabroux, J.C., 1995. The volatile source and magma degassing budget of Merapi volcano: evidence from high-temperature gas emissions and crystal melt inclusions. Merapi Volcano Decade International Workshop, Yogyakarta, October.
- Arsadi, E., Suparta, S., Nishimura, S., 1995. Subsurface structure of Merapi inferred from magnetotelluric, gravimetric and geomagnetic surveys. Merapi Volcano Decade International Workshop, Yogyakarta, October.
- Bahar, I., 1984. Contribution à la connaissance du volcanisme indonésien: le Merapi (Centre-Java), cadre structural, pétrologie-géochimie et implications volcanologiques. Thesis Univ. Sci. et Tech. Languedoc, Montpellier, 215 pp.
- Barberi, F., Cassano, E., Torre, P.L., Sbrana, A., 1991. Structural evolution of Campi flagrei caldera in light of volcanological and geophysical data. *J. Volcanol. Geotherm. Res.* 48, 33–49.
- Barnes, D.F., 1966. Gravity changes during the Alaska Earthquake. *J. Geophys. Res.* 31, 451–456.
- Beauducel, F., 1991. Chaîne de contrôle et d'acquisition pour instruments géodynamiques. Report of ECAM, ORB, 49 pp.
- Becker, M., Balestri, L., Bartell, R., Berrino, G., Bonvalot, S., Csapo, G., Diament, M., D'Errico, M., Gerstenecker, C., Gagnon, C., Jousset, P., Kopaev, A., Liard, J., Marson, I., Meurers, B., Nowak, I., Nakai, S., Rehren, F., Richter, B., Schüll, M., Somerhausen, A., Spita, W., Szatmari, S., Van Ruyambeke, M., Wenzel, H.G., Wilmes, H., Zucchi, M., Zürn, W., 1995. Microgravimetric measurements at the 1994 International Absolute Gravimeter Comparison in Sèvres, France. *Metrologia* 32, 145–152.
- Berrino, G., Rymer, H., Brown, G.C., Corrado, G., 1992. Gravity-height correlations for unrest at calderas. *J. Volcanol. Geotherm. Res.* 53, 11–26.
- Berthommier, P., 1990. Etude volcanologique du Merapi (Centre Java): Téphrostratigraphie et Chronologie—produits éruptifs. Thesis Univ. B. Pascal—Clermont-Ferrand II, 223 pp.
- Berthommier, P., Camus, G., Condomines, M., Vincent, P., 1990. Le Merapi (Centre-Java): Elements de chronologie d'un strato-volcan andésitique. *C.R. Acad. Sci.*, 311 II, 213–218.
- Blake, S., 1984. Volatile oversaturation during the evolution of silicic magma chambers as an eruption trigger. *J. Geophys. Res.* 89, 8237–8244.
- Bonafede, M., 1990. Axi-symmetric deformation of a thermo-poroelastic half-space: inflation of a magma chamber. *Geophys. J. Int.* 103, 289–299.
- Bonafede, M., Olivieri, M., 1995. Displacement and gravity anomaly produced by a shallow vertical dyke in a cohesionless medium. *Geophys. J. Int.* 123, 639–652.
- Bonvalot, S., Metaxian, J.Ph., Gabalda, G., Perez, O., 1995. Gravity and GPS studies at Masaya Volcano (Nicaragua): crustal structure modelling and monitoring volcanic activity. IUGG, 75th Anniversary of the IUGG, Boulder, CO, 2–14 July.
- Bonvalot, S., Diament, M., Deplus, C., G. Gabalda, P., 1996. Bachèlery. Second EVOP Workshop, 2–4 May. Santorini island, Greece.
- Brandeis, G., Jaupart, C., 1987. Crystal sizes in intrusions of different dimensions: constraints on the cooling regime and the crystallisation kinetics. *Magmatic Proc.: Physicochem. Principles* 1, 307–318.
- Brown, G.C., Rymer, H., Thorpe, R.S., 1987. The evolution of andesite volcano structures: new evidence from gravity studies in Costa Rica. *Earth Planet. Sci. Lett.* 82, 323–334.
- Brown, G., Everett, S.P., Rymer, H., McGarnie, D.W., Foster, I., 1991. New light on caldera evolution—Asjka, Iceland. *Geology* 19, 352–355.
- Budetta, G., Carbone, D., 1997. Potential application of the Scintrex CG3-M gravimeter for monitoring volcanic activity: results of fields trials on Mt. Etna, Sicily. *J. Volcanol. Geotherm. Res.* 76, 199–214.
- Burnham, C.W., 1979. The importance of volatile constituents. In: Yoder, H.S. (Ed.), *The Evolution of Igneous Rocks*. Princeton University Press, Princeton, NJ, pp. 439–482.
- Camacho, A.G., Vieira, R., de Toro, C., 1991. Microgravimetric model of the Las Canadas caldera (Tenerife). *J. Volcanol. Geotherm. Res.* 47, 75–88.
- Camus, G., Gourgaud, A., Mossand-Berthommier, P.C., Vincent, P.M., 2000. Merapi (Central Java, Indonesia): an outline of the structural and magmatological evolution, with a special emphasis to the major pyroclastic events. *J. Volcanol. Geotherm. Res.* 100, 139–163.
- Cartwright, D.E., Tayler, R.J., 1971. New computations of the tide-generating potential. *Geophys. J. R. Astron. Soc.* 23, 45–74.
- Christiansen, R.L., Peterson, D.W., 1981. Chronology of the 1980 eruptive activity. In: *The 1980 eruptions of Mount St Helens*, Washington, DC. U.S. Geol. Surv., Prof. Pap. 1250, 525–540.
- Chueca, R., Ducarme, B., Melchior, P., 1985. Preliminary investigation about a quality factor for tidal gravity stations. *Bull. Inform. Marées Terrestres* 94, 6334–6337.
- Davis, P.M., 1986. Surface deformation due to inflation of an arbitrary oriented triaxial ellipsoidal cavity in an elastic half-space, with reference to Kilauea volcano, Hawaii. *J. Geophys. Res.* 91, 7429–7438.
- De la Cruz-Reyna, S., Mena, M., Espinola, J.M., 1986. Observed gravity change in the epicentral area of the Oaxaca, Mexico 1978 Earthquake. *Earthq. Predict. Res.* 4, 111–119.
- De Mets, C., Gordon, R.G., Argus, D.F., Stein, 1990. Current plate motion. *Geophys. J. Int.* 101, 425–478.

- De Meyer, F., Ducarme, B., Elwahabi, A., 1995. Continuous gravity observations at Mount Etna (Sicily). IUGG XXI General Assembly, Boulder, CO, 2–14 July.
- Deplus, C., Bonvalot, S., Dahrin, D., Diament, M., Harjono, H., Dubois, J., 1995. Inner structure of the Krakatau Volcanic Complex (Indonesia) from gravity and bathymetry data. *J. Volcanol. Geotherm. Res.* 64, 23–52.
- Dowden, J., Murray, J., Kapadia, P., 1995. Mathematical modelling of the stress regime in Mount Etna using ground deformation measurements 1987–1992. *Tectonophysics* 249, 141–154.
- Dvorak, J., Pardyanto, L., Matahelumual, J., 1982. Scientific results of the VSI-USGS cooperative volcanological program (January 1982 to June 1982) unpublished data. U.S. Geol. Surv. Open File Report 84-20.
- Dwipa, S., Yohana, T., Jousset, P., Diament, M., 1994. The role of gravity in volcanology. National Gravity Seminar.
- Dzurisin, D., Koyanagi, R.Y., English, T.T., 1984. Magma supply and storage at Kilauea volcano, Hawaiï, 1956–1983. *J. Volcanol. Geotherm. Res.* 21, 177–206.
- Dzurisin, D., Anderson, L.A., Eaton, G., Konyanagi, R.Y., Lipman, P.W., Lockwood, J.P., Okamura, R.T., Puniwai, G.S., Sako, M.K., Yamashita, K.M., 1980. Geophysical observations of Kilauea volcano, Hawaii. 2. Constraints on the magma supply during November 1975–September 1977. *J. Volcanol. Geotherm. Res.* 7, 241–269.
- Eggers, A.A., 1983. Temporal gravity and elevation changes at Pacaya volcano, Guatemala. *J. Volcanol. Geotherm. Res.* 19, 233–237.
- Eggers, A.A., 1987. Residual gravity changes and eruption magnitude. *J. Volcanol. Geotherm. Res.* 33, 201–216.
- Farrell, W.E., 1972. Deformation of the Earth by surface loads. *Rev. Geophys. Space Phys.* 10, 761–797.
- Francis, O., Dehant, V., 1987. Recomputation of Green's functions for loading estimations. *Bull. Inf. Marees Terrestres* 100, 6962–6986.
- Froger, J.L., Bonneville, A., Mulyadi, E., 1992. Signature gravimétrique des caldeiras et des chambres magmatiques associées. Exemple du volcan Tenger (Java Est), C.R. Acad. Sci. Paris, 315, II, pp. 749–755.
- Goodkind, J.M., 1986. Continuous measurement of nontidal variations of gravity. *J. Geophys. Res.* 91 (B9), 9125–9134.
- Hagiwara, Y., 1977. The Mogi model as a possible cause of the crustal uplift in the eastern part of Uzu Peninsula and the related gravity change. *Bull. Earthq. Res. Inst., Uni. Tokyo* 52, 301–309.
- Hagiwara, Y., 1977. Gravity changes associated with seismic activity. In: Kisslinger, C., Suzuki, Z. (Eds.), *Earthquake Precursor*, vol. 2. AEPS, pp. 137–146.
- Hammer, J., Cashman, K.V., 1995. A textural analysis of 1986–1994 Merapi dome lavas and pyroclasts from the 1994 eruption. Merapi Decade Volcano International Workshop, Yogyakarta, October.
- Hammer, J.E., Cashman, K.V., Voight, B., 2000. Magmatic processes revealed by textural and compositional trends in Merapi dome lavas. *J. Volcanol. Geotherm. Res.* 100, 165–192.
- Hugill, A., 1984. The design of a gravimeter with automatic read-out. Thesis, Flinders University of South Australia.
- Hunt, T.M., Kissling, W.M., 1994. Determination of reservoir properties at Wairakei geothermal field using gravity change measurements. *J. Volcanol. Geotherm. Res.* 63, 129–143.
- Hutchison, C.S., 1976. Indonesian active volcanic arc: K, Sr, and Rb variation with depth to the Benioff zone. *Geology* 4, 407–408.
- Iida, K., Hayakawa, M., Katayose, K., 1952. Gravity survey of Mihara volcano, Ooshima Island and changes in gravity caused by eruptions. *Geol. Surv. Jpn. Rep.* 152, 1–28 (in Japanese with English abstract).
- Ishihara, K., 1990. Pressure sources and induced ground deformation associated with explosive eruptions at an andesitic volcano: Sakurajima volcano, Japan. In: Ryan, M.P. (Ed.), *Magma Transport and Storage*, pp. 336–353.
- Jachens, R.C., Eaton, G.P., 1980. Geophysical observations of Kilauea volcano, Hawaii. 1. Temporal gravity variations related to the 29 November 1975, $M = 7.2$. Earthquake and associated summit collapse. *J. Volcanol. Geotherm. Res.* 7, 225–240.
- Jachens, R.C., Roberts, C.W., 1985. Temporal and areal gravity investigations at Long Valley Caldera, California. *J. Geophys. Res.* 90, 11 210–11 218.
- Jachens, R.C., Thatcher, W., Roberts, C.W., Stein, R.S., 1983. Correlation of changes in gravity, elevation and strain in Southern California. *Science* 219, 1215–1217.
- Jachens, R.C., Spydell, D.R., Pitts, G.S., Dzurisin, D., Roberts, C.W., 1984. Temporal gravity and elevation changes at Mt St Helens, March–May 1980. In: Lipman, P.W., Mullineaux, D.R. (Eds.), *The 1980 eruptions of Mount St Helens, Washington, DC*. U.S. Geol. Surv., Prof. Pap. 1250, 175–182.
- Jahr, T., Jentzsch, G., Diaó, E., 1995. Microgravity measurements at Mayon volcano Luwón, Philippines. *Conseils de l'Europe—Cahiers de l'E.C.G.S.* 8, 307–317.
- Jaupart, C., Allègre, C., 1991. Gas content, eruption rate and instabilities of eruption regime in silicic volcanoes. *Earth Planet. Sci. Lett.* 102, 413–429.
- Jaupart, C., Tait, S., 1995. Dynamics of differentiation in magma reservoirs. *J. Geophys. Res.* 100, 17 615–17 636.
- Johnsen, G.V., Björnsson, A., Sigurdsson, 1980. Gravity and elevation changes caused by magma movement beneath the Krafla Caldera, NorthWest Iceland. *J. Geophys.* 47, 132–140.
- Johnson, D.J., 1987. Elastic and inelastic magma storage at Kilauea Volcano. U.S. Geol. Surv. Prof. Pap. 1350, 1297–1306.
- Jousset, P., 1996. Gravimétrie et microgravimétrie en volcanologie: méthodologie et application au volcan Merapi, Java, Indonésie. PhD Univ. Paris VII-IPGP.
- Jousset, P., Van Ruymbeke, M., Bonvalot, S., Diament, M., 1995. Performance of two Scintrex meters at the Fourth International Comparison of Absolute Gravimeters. *Metrologia* 32, 231–244.
- Jousset, P., A. Suzuki, T. Maekawa, H. Mori, H. Okada, 1997. Microgravity and deformation measurements at volcanoes in Hokkaido. *Jap. Earth Plan. Sci. Joint Meeting*, 25–28 March, Nagoya.
- Katili, J.A., 1974. Volcanism and plate tectonics in the Indonesian Islands arc. *Tectonophysics* 26, 165–188.
- Kreyszig, E., 1988. *Advanced Engineering Mathematics*, 6th Ed. Wiley, New York, 1294 pp.
- Laesapura, A., 1994. Etude gravimétrique du volcan Merapi, Java,

- Indonésie. Rapport de DEA de Géophysique Interne de l'IPGP., 23 pp.
- Lambert, A., Beaumont, C., 1977. Nano variations in gravity due to seasonal groundwater movements: implications for the gravitational detection of tectonic movements. *J. Geophys. Res.* 82 (2), 297–306.
- Lee, T.Y., Lawver, L.A., 1995. Cenozoic plate reconstruction of southeast Asia. *Tectonophysics* 251, 85–138.
- Le Provost, C., Lyard, F., 1993. Towards a detailed knowledge of the World Ocean Tide: the example of Kerguelen Plateau. *Geophys. Res. Lett.* 20, 1519–1522.
- Longman, I.M., 1959. Formulas for computing the tidal accelerations due to the Moon and the Sun. *J. Geophys. Res.* 64 (12), 2351–2355.
- Malone, S.D., Frank, D., 1975. Increased heat emission from Mount Baker, Washington. *Trans. Am. Geophys. Union* 56, 679–685.
- McDonald, G.A., 1972. *Volcanoes*. Prentice-Hall, Englewood Cliffs, NJ.
- McKee, C., Mori, J., Talai, B., 1989. Microgravity changes and ground deformation at Rabaul Caldera, 1973–1985. In: J.H. Latter (Ed.), *IAVCEI Proceedings in Volcanology 1*. pp. 399–428.
- Melchior, P., 1989. The phase lag of Earth tides and the braking of the Earth's rotation. *Phys. Earth Planet. Inter.* 56, 186–188.
- Melchior, P., Francis, O., Ducarme, B., 1995. Tidal gravity measurements in SouthEast Asia. IUGG XXI General Assembly, Boulder, CO, 2–14 July.
- Merriam, J.B., 1992. Atmospheric pressure and gravity. *Geophys. J. Int.* 109, 488–500.
- Metaxian, J.P., 1994. Etude sismologique et gravimétrique d'un volcan actif: dynamisme interne et structure de la Caldera Masaya, Nicaragua. PhD, Université de Savoie, 200 pp.
- Mogi, K., 1958. Relations between the eruptions of various volcanoes and the deformations of the ground surfaces around them. *Bull. Earthq. Res. Inst. Univ. Tokyo* 36, 99–134.
- Molodensky, M.S., 1961. The theory of nutations and diurnal Earth tides. *Ive Symp. Intern. Marées Terr. Comm. Obs. Roy. Belg.*, 188, S. *Géophys.* 58, 25–56.
- Naozaki, K., Kajiwara, T., Hayashi, K., 1990. Scintrex technical information, Scintrex Ltd publ.
- Newhall, C., Bronto, S., Alloway, B.V., Andreastuti, S., Banks, N.G., Bahar, I., Del Marmol, M.A., Hadisantono, R.D., Holcomb, R.T., McGeehin, J., Miksic, J.N., Rubin, M., Sayudi, S.D., Sukhyar, R., Tilling, R.I., Torley, R., Trimble, D., Wirakusumah, A.D., 2000. 10,000 Years of explosive eruptions at Merapi Volcano, Central Java: Archaeological and modern implications. *J. Volcanol. Geotherm. Res.* 100, 9–50.
- Niebauer, T.M., 1988. Correcting gravity measurements for the effects of local air pressure. *J. Geophys. Res.* 93 (B7), 7989–7991.
- Ratdomopurbo, A., 1995. Etude sismologique du volcan Merapi et formation du dôme de 1994. Thesis Univ. Joseph Fourier, 208 pp.
- Ratdomopurbo, A., Poupinet, G., 1995. Seismicity of the Merapi volcano: evidence for the existence of two mechanisms of magma overpressure development. Merapi Decade Volcano International Workshop. 5–9 October, Yogyakarta.
- Ratdomopurbo, A., Poupinet, G., 2000. An overview of the seismicity of Merapi volcano (Java, Indonesia). *J. Volcanol. Geotherm. Res.* 100, 193–214.
- Rothacher, M., Gerhard, G., Gurtner, W., Brockmann, E., Mervart, L., 1993. Bernese GPS Software Version 3.4. Universität Bern Astronomisches Institut.
- Rousset, D., Lesquer, A., Bonneville, A., Lénat, J.F., 1989. Complete gravity study of Piton de la Fournaise volcano, Réunion Island. *J. Volcanol. Geotherm. Res.* 36, 37–52.
- Ruegg, J. C., Bougault, C., 1992. AG3D: 3D Geodetic Adjustment program, IGP, unpublished.
- Rundle, J.B., 1978. Gravity changes and the Palmdale uplift. *Geophys. Res. Lett.* 5, 41–44.
- Rydelek, P.A., Zürn, W., Hinderer, J., 1991. On tidal gravity, heat flow and lateral heterogeneities. *Phys. Earth Planet. Inter.* 68, 215–229.
- Rymer, H., 1994. Microgravity change as precursor to volcanic activity. *J. Volcanol. Geotherm. Res.* 61, 311–328.
- Rymer, H., Brown, G.C., 1986. Gravity fields and the interpretation of volcanic structures: geological discrimination and temporal evolution. *J. Volcanol. Geotherm. Res.* 27, 229–254.
- Rymer, H., Brown, G.C., 1987. Causes of microgravity change at Poas volcano, Costa Rica: an active but non-eruptive system. *Bull. Volcanol* 49, 389–398.
- Rymer, H., Brown, G., 1989. Gravity changes as a precursor to volcanic eruption at Poas volcano, Costa Rica. *Nature* 342, 902–905.
- Rymer, H., Tryggvason, E., 1993. Gravity and elevation changes at Askja, Iceland. *Bull. Volcanol.* 55, 362–371.
- Rymer, H., Murray, J.B., Brown, G.C., Ferruci, F., McGuire, W.J., 1993. Mechanisms of magma eruption and emplacement at Mt Etna between 1989 and 1992. *Nature* 361, 439–441.
- Sanderson, T.J.O., 1982. Direct gravimetric detection of magma movements at Mount Etna. *Nature* 297, 487–490.
- Schwiderski, E.W., 1980. On charting global ocean tides. *Rev. Geophys. Space Phys.*, 18.
- Seigel, H.O., Brcic, I., Mistry, P., 1990. The CG3-M—a high precision, microgal resolution, land gravimeter, with world-wide range. Sidik, M., 1989. Penyelidikan kakas gravitasi di Gunung Merapi, Gunung Merbabu dan sekitarnya. Report of Gadjah Mada University, Yogyakarta, Indonesia, 165 pp.
- Smith, R.B., Reilinger, R.E., Meertens, C.M., Hollis, J.R., Holdhal, S.R., Dzursin, D., Gross, W.K., Klingele, E.E., 1989. What's moving at Yellowstone?. *EOS* 70, 113–125.
- Smith, W.H.F., Wessel, P., 1990. Gridding with continuous curvature splines in tension. *Geophysics* 55, 293–305.
- Sukhyar, J., 1995. Learning from 22 November 1994 Merapi Eruption. Merapi Decade Volcano International Workshop, 5–9 October, Yogyakarta.
- Sun, H.P., Ducarme, B., Dehant, V., 1995. Theoretical calculation of atmospheric gravity Green's function. *Conseils de l'Europe—Cahiers de l'E.C.G.S.* 11, 223–237.
- Tait, S., Jaupart, C., Vergnole, S., 1989. Pressure, gas content and eruption periodicity of a shallow, crystallising magma chamber. *Earth Planet. Sci. Lett.* 92, 107–123.
- Tarantola, A., Valette, B., 1982. Generalized nonlinear inverse problems solved using the least squares criterion. *Rev. Geophys. Space Phys.* 20, 219–232.

- Tilling, R., 1989. Measures of little gravity. *Nature* 342, 862–863.
- Tjetjep, W., 1995. Mitigation and volcanic eruption in Indonesia. Merapi Decade Volcano International Workshop, Yogyakarta, October.
- Torge, W., 1981. Gravity and height variations connected with the current rifting episode in Northern Iceland. *Tectonophysics* 71, 227–240.
- Untung, M., Sato, Y., 1978. Gravity and geological studies in Java, Indonesia. Special publication, GSI and GSJ, Joint research program on regional tectonics.
- Van Ruymbeke, M., 1991. New feed-back electronics for LaCoste–Romberg gravimeters. *Conseil de l'Europe—Cahiers du C.E.E.G.S.* 4, 333–337.
- Van Ruymbeke, M., D'Oreye, N., Somerhausen, A., Grammatica, N., 1994. Technological approach from Walferdange to Lanzarote: the EDAS concept. EEC-CEC-DGXII-Environment program: Teide: european laboratory volcano.
- Van Ruymbeke, M., Beauducel, F., Somerhausen, A., 1997. The Environmental Data Acquisition System (EDAS) developed at the Royal Observatory of Belgium, *Cahiers du Centre Européen de Géodynamique et de Sismologie*.
- Venedikov, A.P., 1966. Une méthode pour l'analyse des marées terrestres à partir des enregistrements de longueur arbitraire. *Comm. Obs. Roy. Belg.* 250 SG 71, 437–459.
- Voight, B., Young, K.D., Ratdomopurbo, A., Subandrio, Sajiman, Miswanto, Paijo, Suharno, Bronto, S., 1994. Summit deformation at an island-arc stratovolcano: correlation to lava dome growth and seismicity, Merapi Volcano, Java, Indonesia. *Geol. Soc. Am. Abstracts with Programs*, 26:7, A-483.
- Voight, B., Young, K.D., Ratdomopurbo, A., 1995. A classification of Earthquakes at Merapi Volcano, Java, with comments on causative processes. Merapi Decade Volcano International Workshop, Yogyakarta, October.
- Wahyudi, 1986. Penyelidikan gaya berat di Gunung Merapi. Report of Gadjah Mada Univ., Yogyakarta, Indonesia, 136 pp.
- Watermann, H., 1957. Über systematische Fehler bei Gravimetermessungen. *DGK, München*, 21 (C).
- Wawan, G.A.K., 1985. Analisa gayaberat anomaly udar-bebas Gunung Merapi dan sekitarnya. Report of Gadjah Mada Univ., Yogyakarta, Indonesia, 122 pp.
- Williams, H., McBirney, A.R., 1979. *Volcanology*. Freeman, Cooper & Co, San Francisco, CA, 397 pp.
- Wong, T.F., Walsh, J.B., 1991. Deformation-induced gravity changes in volcanic regions. *Geophys. J. Int.* 106, 513–520.
- Yokoyama, I., 1989. Microgravity and height changes caused by volcanic activity: four Japanese examples. *Bull. Volcanol.* 51, 333–345.
- Yokoyama, I., Hadikusumo, D., 1969. A gravity survey on the Krakatau Islands, Indonesia. *Volcanological survey of Indonesian volcanoes, part 3. Bull. Earth. Res. Inst.* 47, 991–1001.
- Yokoyama, I., Suryo, I., Nazhar, B., 1970. *Volcanological Survey of Indonesian Volcanoes, Pt. 4, Gravity Survey in Central Java. Earthq. Res. Inst. Bull.* 48, 317–329.
- York, D., 1966. Least-squares fitting of a straight line. *Can. J. Phys.* 44, 1079–1086.
- Young, K.D., Voight, B., 1995. Ground deformation studies at Merapi Volcano, Indonesia, Merapi Decade Volcano International Workshop, Yogyakarta, October.
- Young, K.D., Voight, B., Marso, J., Subandrio, Sajiman, Miswanto, Paijo, Suharno, Bronto, S., 1994. Tilt monitoring, lava dome growth and pyroclastic flow generation at Merapi volcano, Java, Indonesia. *Geol. Soc. Am. Abstr. Prog.* 26 (7), A483.
- Zen, Jr., M.T., 1993. Déformation de l'avant-arc en réponse à une subduction à convergence oblique. Exemple de Sumatra. Thesis, Univ. Paris VII, 253 pp.